Egypt. J. Chem. **Vol. 66**, No. 7 pp.63 - 85 (2023)

Egyptian Journal of Chemistry

http://ejchem.journals.ekb.eg/

Impacts of Chemical Reaction and Electric Field with Cattaneo – Christov Theories on Peristaltic Transport of a Hyperbolic Micropolar Nanofluid

Nabil T. M. El-Dabe, Mohamed Y. Abou-zeid, Doaa R. Mostapha, Yasmeen M. Mohamed and Mahmoud E. Oauf

Department of Mathematics, Faculty of Education, Ain Shams University, Roxy, Cairo, Egypt

Abstract

The current investigation described the influences of Cattaneo – Christov heat flux, Soret and Dufour, Hall current. The vertical alternating current produces an electric field is applied on the peristaltic flow of non - Newtonian micropolar nanofluid. The fluid flows inside a tapered stenosed artery. The non – Newtonian fluid obeys the tangent hyperbolic model. The effects of heat generation absorption, joule heating, thermal radiation, chemical reaction, and the permeability of the porous medium are imposed. The slip velocity and thermal slip conditions are assumed. The convective conditions for nanoparticles concentration as well as concentration are constructed. The coupled differential systems of equations yield Soret and Dufour feature. The assumption of the long wavelength with low Reynolds number is employed to simplify the governing equations of fluid motion to be ordinary differential equations. Furthermore, the obtained analytical solutions of these equations are based mainly on applying regular perturbation method together with homotopy perturbation method (HPM). The impacts of the various physical parameters on the axial velocity, spin velocity, temperature, nanoparticles concentration and concentration are illustrated and drawn graphically via a set of graphs. It is noticed that the velocity dwindled with an enriching in the magnitudes of both Hartman number, and electromagnetic parameter. Whereas, the axial velocity elevates with an enlargement in Darcy number, tapering angle, and Hall parameter. Moreover, the spin velocity declines with the increment in the microrotation parameter. Also, it is found that the escalating in thermal relaxation time causes a decaying impact on the temperature. Furthermore, enhancement in the nano Biot number leads to a declination in the magnitude of nanoparticles concentration. The current analytical study is very significant in several medical implementations, like the gastric juice motion in the small intestine when an endoscope is inserted through it.

Keywords: Cattaneo – Christov heat flux; Hall current; Electrohydrodynamics; Stenosis; Micropolar; Nanofluid.

1. Introduction

Micropolar fluids theorem is first represented by Eringen [1]. He recognized that every volume of material element that can rotate independently of the motion of microvolume. These kinds of fluids are deemed as a popularization corresponding to the Navier–Stokes equation. In the physical visualization, these fluids could symbolize to the fluids which containing rigid, randomly amended elements roaming in a viscous medium. Also, the deviation of fluid particles is ignored. The numerical model, that elucidates the whole angular velocity field of the particles rotation, is primary depend on the inserting of a new vector field named as the micro-rotation. Therefore, a new additive equation that displays the law of angular momentum (spin velocity) is appeared. This theory has been felicitously discussed by several researchers in various theoretical studies of fluid dynamics see Refs. [2-7].

Heat and mass transfer is deemed a joint phenomenon that plays a primary important role in several engineering as well as industrial processes, such as heat exchangers, equipment power collectors, food processing and so. Also, temperature gradients are responsible for occurring heat flux. It has many different applications like in cooling processes, thermal regulation in electronic devices, and nuclear reactors. Many researchers employed the theories of convectional transfer in their theoretical studies. Nevertheless, these convectional theories are

* Corresponding author should be addressed yasmeenmostafa@edu.asu.edu.eg ; **(Yasmeen M. Mohamed).**
EJCHEM use only: Received date 26 September 2022; revised date 10 October 2022; accepted date 12 October 2022
DOI: 10.21608/EJCHEM.2022.165317.7033

considered to be insufficient because of wave propagation's infinite speed. The law related to heat conduction in addition to the several properties of heat transfer is firstly introduced by Fourier [8]. Thus, Cattaneo [9] modulate a conventional law of Fourier to involve thermal relaxation time (known as non - Fourier law). This added term elucidates the time needed of the medium to transport heat to its frontier particles. Fourier's heat idiom is deemed to be a parabolic energy equation. Meanwhile, Cattaneo's equation causes hyperbolic type energy equation. The model of Cattaneo is amended by Christov [10]. Similarly, Fick's law for diffusion plays an eloquent role for analysing mass transport. For more realistic modelling, this law was modulated with the CC model (also called non-Fick model) [11]. In recent years, there are several essential analysis studies which scrutinized theoretically the CC model are cited in [12-17].

Lately, several essential studies concerned in displaying and analysing the fluid flow in the case of low fluid density and strong magnetic field. The conductivity is decreased because of utilizing a strong magnetic field together with low density This indicates to an induced current, which is named as the Hall current. This electromagnetic phenomenon (Hall currents) has an essential significant role in engineering, mechanics, and biomechanics implementations. These implementations are, Hall impact sensors, coils refrigeration, Hall accelerators, magneto-meters, electric processors, Hall actuators, spacecraft propulsion, etc. [18-20]. Studying the interactions between an electric field and a flow field is defined as electro-hydrodynamics (EHD). Also, it is known as electro - kinetics or electro-fluid-dynamics (EFD). EHD has many various significant applications in the fields of engineering, biomechanics, microfluidic devices, plasma actuators, enrichment of drying rates, drag reduction, gas pumps, micro-electro-mechanical systems (MEMS), biomedical diagnostic instruments, biochemical analysis, chemical devices and biomedical devices. The constitutive equations of motion elated to electrohydrodynamic can be divided into two combinations. The first one is the equations of hydrodynamic, the second one is the electric field equations. EHD has been investigated through several theoretical studies see [21-24].

Blood is deemed as the most significant biological fluid. According to its elastic quaff it may regarded as a non-Newtonian fluid. Deformable saturation of red blood cells is responsible for this elastic nature. Stenosis is regarded as one of the most rife arterial diseases. it is denoted as narrowing of anybody passage. The existence of a stenosis in the artery caused a changing in the nature of the blood flow. Therefore, the state of the blood is converted from normal state to troubled one. Several diseases like heart failure by reducing or occluding the blood supply, myocardial infarction, cardiovascular are caused by the existence of arterial stenosis. There are many biological studies that displayed the mechanism of blood flow in the existence of stenosed tapered artery, see [25-30]. It is very intricate to treat the equations govern the motion in the existence of nonlinear terms. These terms manifest in the equations of motion as a reason of the flow demeanour of non-Newtonian nanofluids flow together with Cattaneo-Christov heat and mass fluxes. Thus, the exact solutions of this kind of problems are virtually impossible. Therefore, numerical solutions for this sort of problems have been obtained through several theoretical studies [31-33]. The main target is turned to obtain a semi analytical (approximate) solution with the help of conventional perturbation technique in addition to homotopy perturbation method (HPM). After utilizing these approximate methods, the resultant nonlinear differential equations and their corresponding boundary conditions are transformed into another simple system of equations which can be treated easily.

In accordance with above aforesaid, it is noticed that the study of the impacts of Cattaneo-Christov heat flux and mass fluxes inside a tapered stenosed artery on the peristaltic motion in the existence of nonfluid phenomenon has not been discussed yet. Consequently, the essential significant of this article is to study of peristaltic motion of hyperbolic tangent micropolar nanofluid. The influences of Cattaneo-Christov double diffusion through stenosed porous artery are taken into our consideration. In addition, the impacts of Hall currents as well as ohmic dissipation in the existence of electric field are imposed. The influences of thermal radiation, Soret and Dufour impacts, heat generation and chemical reaction are also included. The slip condition for temperature distribution and convective conditions for both distributions of concentration as well as nano phenomenon are presupposed. The mathematical intricacy of our study can be alleviating by applying the long wavelength and low Reynolds number presumptions. These non-linear equations are analytically disbanded by applying the conventional perturbation method together with homotopy perturbation method up to the first order. The influences of diverse physical parameters on the various distributions are analysed numerically and displayed through a set of graphs.

The temple of this theoretical study can be implemented as follows: Sec.2 clarifies the

mathematical formulation of the problem. The equations govern the motion of the considered system are introduced through Sec.3. Sec.4 displays the methodology of solutions. The numerical results of the diverse physical parameters on the various distributions are debated though Sec.5. Sec. 6 encompasses the discussion of the trapping phenomenon. Finally, summarized results of the present study are displayed in Sec. 7.

2. Mathematical formulation of the problem

Consider two-dimensional peristaltic flow of an incompressible tangent hyperbolic micropolar nanofluid stream inside a horizontal co–axial tubes. The outer tube is tapered and has a sinusoidal wave traveling down its wall in the presence of mild stenosis. Whilst the inner one is rigid, uniform, and moving with a constant speed (see Fig. 1). The system is stressed by strong magnetic field of uniform strength. Nevertheless, radial alternating current electric field is also presupposed. The outer tube is grounded, and the inner one is kept at the electric potential. Whereas the influence of Hall current is introduced. The cylindrical polar coordinate system in the fixed frame of refence is employed, with the axis coincides with the axis of the tubes. Hall current generates a force in direction because of the impact of strong magnetic field. Therefore, the flow becomes in three dimensions. The convective mass as well as convective nanoparticles conditions are influenced. Moreover, it is presupposed that the inner tube at is maintained at constant temperatures nanoparticles concentration and concentration. Meanwhile, the outer one at is heated by a temperature nanoparticles concentration and concentration. Influences chemical reaction, Soret and Dufour are also presumed. The magnetic Reynolds number is chosen to be very small. Thus, the induced magnetic field is modicum when compared with the applied magnetic field. Therefore, the induced magnetic field is ignored. The thermal slip condition is also imposed.

The effective radius of the tapered artery $R_s(z)$, can be written as follows:

$$R_s(z)=\begin{cases} R_0-\delta_s m_0(Z+L_0+d_0) & -L_0\le Z\le z_0 \\ R_0-\delta_s m_0(Z+L_0+d_0)-\dfrac{H_0}{2}\left(1+\cos\left(\dfrac{\pi}{Z_0}Z\right)\right) & -z_0\le Z\le z_0 \\ R_0-\delta_s m_0(Z+L_0+d_0) & z_0\le Z\le d_0 \end{cases} \quad (1)$$

where, $H_0=h_s\cos\omega$ is named as the height of the stenosis inside the tapered outer tube, $m_0=\tan\omega$ is defined as the slope of the tapered artery, h_s is denoted as the maximum height of the stenosis, ω is known as the tapering angle. In this analytical study, we analyze and discuss all the conceivable cases for diverse tube shapes: the case when ω take a negative value $(\omega<0)$ is denoted as converging tapering case, when setting $(\omega=0)$ one can obtain the case which named non-tapered artery, at the end , diverging tapering case can be caused for positive values of ω i.e. $(\omega>0)$ [24].

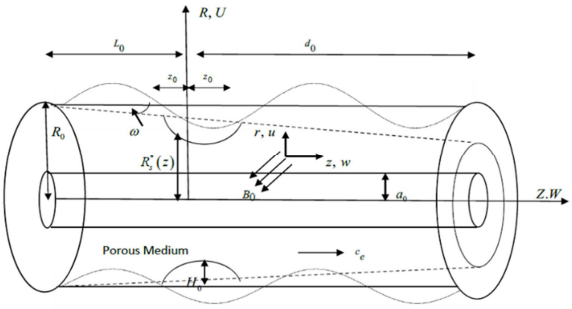

Fig. 1. Diagram of fluid influx

The geometry of the peristaltic wall's surface may be represented by the following expressions [30]:

$$H_1(Z,t)=a_1\cos\frac{2\pi}{\lambda}\left(Z-\frac{k}{R_0}t\right), \quad (2)$$

The equations of the radii can be represented by the following expressions [11, 20, and 27]:

$$\left.\begin{aligned} R_{s1}&=a_0 \\ R_{s2}&=R_s(z)+H_1 \end{aligned}\right). \quad (3)$$

The constitutive equation of Cauchy stress tensor $\underline{\tau}^h$ for tangent hyperbolic fluid model can be presented as follows:

$$\underline{\tau}^{h} = -\mathrm{P}_{e}\ \mathrm{I} + \underline{S}_{H},$$
(4)

$$\underline{S}_{H} = \left[\mu_{\infty h} + \left(\mu_{\infty h} + \mu_{0h}\right)\tanh\left(\varpi\dot{\vec{\xi}}\right)^{n}\right]\underline{A}_{1h}, \quad (5)$$

$$\dot{\vec{\xi}} = \sqrt{\frac{1}{2}\Theta_{h}}, \qquad \Theta_{h} = tr\left(\underline{A}_{1h}^{2}\right),$$
(6)

$$\underline{A}_{1\mathrm{h}} = \left(\nabla\underline{\mathrm{V}}\right) + \left(\nabla\underline{\mathrm{V}}\right)^{\mathrm{T}}.$$
(7)

Consider the case when $\mu_{\infty h} = 0$, and $\varpi\dot{\vec{\xi}} \gg 1$. Therefore, the element of extra stress tensor may be inscribed as follows:

$$\underline{S}_{H} = \mu_{0h}\left(1 + n_{h}\left(\varpi\dot{\vec{\xi}} - 1\right)\right)\underline{A}_{1h}.$$
(8)

The velocity components, temperature, electric potential, nanoparticles concentration and concentration may be written as follows:

$$\underline{V} = \left(U\left(R,\theta,Z;t\right), W\left(R,\theta,Z;t\right), 0\right),$$
$$T = T\left(R,\theta,Z;t\right),\ \varphi = \varphi\left(R,\theta,Z;t\right),$$
$$f = f\left(R,\theta,Z;t\right), \quad \text{and} \quad C = C\left(R,\theta,Z;t\right).$$
(9)

Postulate that the tube length is an integral multiple of wavelength λ_{0}. Also, the pressure difference through the ends of the outer tube is constant. So, the unsteady flow in fixed frame $\left(R,\theta,Z\right)$ transformed to steady flow in the wave frame $\left(r,\theta,z\right)$, which moves with velocity $c_{e} = k\left(R_{0}\right)^{-1}$.

The transformation between these two frames of reference can be represented as:

$$z = Z - t\,c_{e},\ r = R,\ w\left(r,z\right) = W\left(R,Z;t\right) - c_{e},$$
$$\text{and}\ \ u\left(r,z\right) = U\left(R,Z;t\right). \quad (10)$$

The body forces of electrical origin per unit volume f_{e} may be represented as [21]

$$f_{el} = \rho_{el}\,\underline{E}_{f} - \frac{1}{2}E_{f}^{2}\nabla\varepsilon + \frac{1}{2}\nabla\left(\rho_{s}E_{f}^{2}\left(\frac{\partial\varepsilon}{\partial\rho_{s}}\right)\right),$$
(11)

where, the first term in Eq. (11) is the ordinary electrostatic volume force (the Coulomb force or the force due to the free charge ρ_{el}). In this study, we assume that there are no volume charges present $\left(\rho_{el} = 0\right)$. Thus, .in this case, the term $\rho_{el}\,\underline{E}_{f}$ can be disregarded. The second term $\frac{1}{2}E_{f}^{2}\nabla\varepsilon$ represents the dielectric force, which depends on the gradient of ε. The last term $\frac{1}{2}\nabla\left(\rho_{s}E_{f}^{2}\left(\frac{\partial\varepsilon}{\partial\rho_{s}}\right)\right)$ is called the electrostriction term which term can be involved in the pressure term.

Since there is no free charge, the Maxwell's equations are [22]:

$$\nabla\cdot\left(\varepsilon\underline{E}_{f}\right) = 0, \quad (12)$$

$$\nabla\wedge\underline{E}_{f} = 0, \ \text{ or } \ \underline{E}_{f} = -\nabla\varphi_{e}. \quad (13)$$

It is presupposed that the dielectric constant ε is a function of the temperature [22], and it can be expressed as:

$$\varepsilon = \varepsilon_{0}\left[1 - e_{0}\left(T - \vartheta_{1}\right)\right], \quad (14)$$

where, e_{0} is denoted as the thermal expansion coefficient of dielectric constant and is assumed to be small and positive, ε_{0} is indicated as the permittivity at vacuum.

The modified pressure may be expressed as:

$$P_{m} = P_{e} - \frac{1}{2}\left(\rho_{s}E_{f}^{2}\left(\frac{\partial\varepsilon}{\partial\rho_{s}}\right)\right). \quad (15)$$

The current density $\underline{J}_{c}$ can be expressed as [3, and 18],

$$\underline{J}_{c} = \sigma_{s}\left[\underline{E}_{f} + \underline{V}\wedge\underline{B} - \frac{1}{en_{e}}\left(\underline{J}\wedge\underline{B}\right)\right]. \quad (16)$$

Energy equation can be inscribed as:

$$(\rho c)_s \frac{dT}{dt} = -\nabla \cdot \underline{q}_H + (\rho c)_n \left[D_N (\nabla T \cdot \nabla f) + \frac{D_T}{\vartheta_2} (\nabla T \cdot \nabla T) \right]$$
$$-\nabla \cdot \underline{q}_r + R_G (T - \vartheta_2) + \frac{DK_H}{C_{ne}} \nabla^2 C + \frac{1}{\sigma_s} (\underline{J} \cdot \underline{J}). \quad (17)$$

Nanoparticles concentration equation can be expressed as:

$$\frac{df}{dt} = -\nabla \cdot \underline{q}_N + \frac{D_T}{\vartheta_2} \nabla^2 T. \quad (18)$$

Cattaneo – Christov double diffusion model:

Cattaneo – Christov heat flux may be introduced as follows [11]:

$$\underline{q}_H + \lambda_H \left[\frac{\partial \underline{q}_H}{\partial t} + \underline{V} \cdot \nabla \underline{q}_H - \underline{q}_H \cdot \nabla \underline{V} + (\nabla \cdot \underline{V}) \underline{q}_H \right] = -K_E \nabla T. \quad (19)$$

Cattaneo-Christov nano flux may be defined as follows [11]:

$$\underline{q}_N + \lambda_N \left[\frac{\partial \underline{q}_N}{\partial t} + \underline{V} \cdot \nabla \underline{q}_N - \underline{q}_N \cdot \nabla \underline{V} + (\nabla \cdot \underline{V}) \underline{q}_N \right] = -D_N \nabla f, \quad (20)$$

which are the modulated Fourier's and Fick's laws. One setting $(\lambda_H = 0)$ and $(\lambda_N = 0)$, it can reduce to the original Fourier's and Fick's laws. Since the fluid is incompressible $(\nabla \cdot \underline{V} = 0)$, Eqs. (14 and 15) may be rewritten as follows:

$$\underline{q}_H + \lambda_H \left[\left(\frac{\partial}{\partial t} + \underline{V} \cdot \nabla \right) \underline{q}_H - \left(\underline{q}_H \cdot \nabla \right) \underline{V} \right] = -K_E \nabla T, \quad (21)$$

$$\underline{q}_N + \lambda_N \left[\left(\frac{\partial}{\partial t} + \underline{V} \cdot \nabla \right) \underline{q}_N - \left(\underline{q}_N \cdot \nabla \right) \underline{V} \right] = -D_N \nabla f. \quad (22)$$

By employment of the Rosseland diffusion flux model, the differential equation for radiative transfer may be converted to a Fourier-kind diffusion equation. It is major to reveal that the Rosseland model is quite delicate in case of thermal radiation (scattering or absorption). The refractive index of the fluid-particle suspension is presumed to be constant. Thus, the nonlinear radiative heat flux may be imposed effectively as [3]:

$$\underline{q}_r = -\frac{4\sigma_0}{3K_r} \frac{\partial T^4}{\partial r}. \quad (23)$$

The temperature differences are assumed to be adequately small. Thus, T^4 can be represented as a linear function of temperature. By using Taylor series expansion for T^4 about the mean fluid temperature T_m and neglecting the higher-order terms, the nonlinear radiative heat flux is reduced to following linear form:

$$T^4 \approx 4T_m^3 T - 3T_m^4. \quad (24)$$

3. The governing equations of fluid motion:

The governing continuity, $r-$ component momentum, $z-$ component momentum, spin velocity, temperature, nanoparticles concentration, concentration and electric potential equations may be written as follows applying Eq. (10):

$$\frac{\partial u}{\partial r} + \frac{u}{r} + \frac{\partial w}{\partial z} = 0, \quad (25)$$

$$\rho_s \left(\mathrm{u} \frac{\partial u}{\partial r} + \mathrm{w} \frac{\partial u}{\partial z} \right) = -\frac{\partial P_m}{\partial r} + \frac{1}{r} \frac{\partial}{\partial r} \left(r \frac{\partial S_{rr}}{\partial r} \right) + \frac{\partial S_{rz}}{\partial z}$$
$$-\frac{S_{\theta\theta}}{r} - K_a \frac{\partial N_m}{\partial z} - \frac{\mu_{0h}}{K_p} u - \frac{\sigma_s B_0}{1+\beta_e^2} \left(\beta_e \frac{\partial \varphi_e}{\partial r} - \frac{\partial \varphi_e}{\partial z} \right)$$
$$-\frac{\sigma_s B_0^2}{1+\beta_e^2} \left(u + \beta_e \left(w + \frac{k}{R_0} \right) \right) + \frac{1}{2} \varepsilon_0 e_0 \left(\frac{\partial T}{\partial r} \right) \left(\frac{\partial \varphi_e}{\partial r} \right)^2$$
$$\frac{1}{2} \varepsilon_0 e_0 \left(\frac{\partial T}{\partial r} \right) \left(\frac{\partial \varphi_e}{\partial z} \right)^2, \quad (26)$$

$$\rho_s \left(\mathrm{u} \frac{\partial w}{\partial r} + \mathrm{w} \frac{\partial w}{\partial z} \right) = -\frac{\partial P_m}{\partial z} - \frac{\mu_{0h}}{K_p} \left(w + \frac{k}{R_0} \right) +$$
$$\frac{\sigma_s B_0}{1+\beta_e^2} \left(-\left(\frac{\partial \varphi_e}{\partial r} + \beta_e \frac{\partial \varphi_e}{\partial z} \right) + B_0 \left(\beta_e u - \left(w + \frac{k}{R_0} \right) \right) \right)$$
$$+ \frac{1}{2} \varepsilon_0 e_0 \left(\frac{\partial T}{\partial z} \right) \left[\left(\frac{\partial \varphi_e}{\partial r} \right)^2 + \left(\frac{\partial \varphi_e}{\partial z} \right)^2 \right] + \frac{1}{r} \frac{\partial}{\partial r} \left(r \frac{\partial S_{rz}}{\partial r} \right)$$
$$+ \frac{\partial S_{zz}}{\partial z} + K_a \left(\frac{\partial N_m}{\partial r} + \frac{N_m}{r} \right), \quad (27)$$

$$\rho_s j_m \left(u \frac{\partial N_m}{\partial r} + \frac{\partial N_m}{\partial z} \right) = -2K_a N_m + K_a \left(\frac{\partial u}{\partial z} - \frac{\partial w}{\partial r} \right)$$
$$+ \gamma_a \left(\frac{\partial^2 N_m}{\partial r^2} + \frac{1}{r} \frac{\partial N_m}{\partial r} + \frac{\partial^2 N_m}{\partial z^2} - \frac{N_m}{r^2} \right),$$

$$(\rho c)_s\left(\mathrm{u}\ \frac{\partial T}{\partial r}+\mathrm{w}\ \frac{\partial T}{\partial z}\right)+\lambda_H\Sigma_H-\frac{16\sigma_0 T_m^3}{3K_r}\left(\frac{\partial^2 T}{\partial r^2}+\frac{1}{r}\frac{\partial T}{\partial r}\right)$$
$$-(\rho c)_n\left[D_N\left(\frac{\partial T}{\partial r}\frac{\partial f}{\partial r}+\frac{\partial T}{\partial z}\frac{\partial f}{\partial z}\right)+\frac{D_T}{\vartheta_2}\left(\left(\frac{\partial T}{\partial r}\right)^2+\left(\frac{\partial T}{\partial z}\right)^2\right)\right]$$
$$-\frac{\sigma_s}{1+\beta_e^2}\left[\left(\frac{\partial \varphi_e}{\partial r}\right)^2+\left(\frac{\partial \varphi_e}{\partial z}\right)^2+2B_0\left(\left(w+\frac{k}{R_0}\right)\frac{\partial \varphi_e}{\partial r}-u\frac{\partial \varphi_e}{\partial z}\right)\right]$$
$$-\frac{\sigma_s}{1+\beta_e^2}\left(B_0^2\left(u^2+\left(w+\frac{k}{R_0}\right)^2\right)\right)-R_G\left(T-\vartheta_2\right)$$
$$-\frac{DK_H}{C_{ne}}\left(\frac{\partial^2 C}{\partial r^2}+\frac{1}{r}\frac{\partial C}{\partial r}+\frac{\partial^2 C}{\partial z^2}\right)=K_E\left(\frac{\partial^2 T}{\partial r^2}+\frac{1}{r}\frac{\partial T}{\partial r}+\frac{\partial^2 T}{\partial z^2}\right), \tag{28}$$

$$\mathrm{u}\ \frac{\partial f}{\partial r}+\mathrm{w}\ \frac{\partial f}{\partial z}-\frac{D_N}{\vartheta_2}\left[\frac{\partial^2 T}{\partial r^2}+\frac{1}{r}\frac{\partial T}{\partial r}+\frac{\partial^2 T}{\partial z^2}\right]$$
$$+\lambda_N\Sigma_N=D_N\left(\frac{\partial^2 f}{\partial r^2}+\frac{1}{r}\frac{\partial f}{\partial r}+\frac{\partial^2 f}{\partial z^2}\right), \tag{29}$$

$$\mathrm{u}\ \frac{\partial C}{\partial r}+\mathrm{w}\ \frac{\partial C}{\partial z}=D\left(\frac{\partial^2 C}{\partial r^2}+\frac{1}{r}\frac{\partial C}{\partial r}+\frac{\partial^2 C}{\partial z^2}\right)$$
$$+\frac{DK_H}{T_m}\left[\frac{\partial^2 T}{\partial r^2}+\frac{1}{r}\frac{\partial T}{\partial r}+\frac{\partial^2 T}{\partial z^2}\right]-L_r\left(C-C_0\right), \tag{30}$$

$$\varepsilon_0\left(1-e_0\left(T-\vartheta_1\right)\right)\left[\frac{\partial^2 \varphi_e}{\partial r^2}+\frac{1}{r}\frac{\partial \varphi_e}{\partial r}+\frac{\partial^2 \varphi_e}{\partial z^2}\right]$$
$$-e_0\varepsilon_0\frac{\partial T}{\partial r}\frac{\partial \varphi_e}{\partial r}-e_0\varepsilon_0\frac{\partial T}{\partial z}\frac{\partial \varphi_e}{\partial z}=0, \tag{31}$$

where,

$$\Sigma_H=-R_G\left(u\frac{\partial T}{\partial r}+w\frac{\partial T}{\partial z}\right)+(\rho c)_s\left[u^2\frac{\partial^2 T}{\partial r^2}+2uw\frac{\partial^2 T}{\partial r\partial z}+w^2\frac{\partial^2 T}{\partial z^2}\right]$$
$$+(\rho c)_s\left[\left(\left(u\frac{\partial u}{\partial r}+w\frac{\partial u}{\partial z}\right)\frac{\partial T}{\partial r}+\left(u\frac{\partial w}{\partial r}+w\frac{\partial w}{\partial z}\right)\frac{\partial T}{\partial z}\right)\right]-$$
$$(\rho c)_n D_N\left(u\left(\frac{\partial^2 f}{\partial r^2}\frac{\partial T}{\partial r}+\frac{\partial^2 T}{\partial r^2}\frac{\partial f}{\partial r}+\frac{\partial^2 f}{\partial r\partial z}\frac{\partial T}{\partial z}+\frac{\partial^2 T}{\partial r\partial z}\frac{\partial f}{\partial z}\right)\right)-$$
$$(\rho c)_n D_N\left(w\left(\frac{\partial^2 f}{\partial r\partial z}\frac{\partial T}{\partial r}+\frac{\partial^2 T}{\partial r\partial z}\frac{\partial f}{\partial r}+\frac{\partial^2 f}{\partial z^2}\frac{\partial T}{\partial z}+\frac{\partial^2 T}{\partial z^2}\frac{\partial f}{\partial z}\right)\right)-$$
$$2(\rho c)_n\frac{D_T}{\vartheta_2^2}\left[\left(u\left(\frac{\partial T}{\partial r}\frac{\partial^2 T}{\partial r^2}+\frac{\partial T}{\partial z}\frac{\partial^2 T}{\partial r\partial z}\right)+w\left(\frac{\partial T}{\partial r}\frac{\partial^2 T}{\partial r\partial z}+\frac{\partial T}{\partial z}\frac{\partial^2 T}{\partial z^2}\right)\right)\right]$$
$$-\frac{DK_H}{C_{ne}}\left[u\frac{\partial^3 C}{\partial r^3}+w\frac{\partial^3 C}{\partial r^2\partial z}+\frac{u}{r}\frac{\partial^2 C}{\partial r^2}-\frac{u}{r^2}\frac{\partial C}{\partial r}+\frac{w}{r}\frac{\partial^2 C}{\partial r\partial z}+u\frac{\partial^3 C}{\partial r\partial z^2}+w\frac{\partial^3 C}{\partial z^3}\right]$$
$$-\frac{\sigma_s B_0^2}{1+\beta_e^2}\left(2u^2\frac{\partial u}{\partial r}+2w\left(w+\frac{k}{R_0}\right)\frac{\partial w}{\partial z}\right)-\frac{\sigma_s B_0^2}{1+\beta_e^2}\left(2uw\frac{\partial u}{\partial z}+2u\left(w+\frac{k}{R_0}\right)\frac{\partial w}{\partial r}\right)$$
$$-\frac{\sigma_s}{1+\beta_e^2}\left(2u\left(\frac{\partial \varphi_e}{\partial r}\frac{\partial^2 \varphi_e}{\partial r^2}+\frac{\partial \varphi_e}{\partial z}\frac{\partial^2 \varphi_e}{\partial r\partial z}\right)\right)-\frac{\sigma_s}{1+\beta_e^2}\left(2w\left(\frac{\partial \varphi_e}{\partial r}\frac{\partial^2 \varphi_e}{\partial r\partial z}+\frac{\partial \varphi_e}{\partial z}\frac{\partial^2 \varphi_e}{\partial z^2}\right)\right)$$
$$-\frac{16\sigma_0 T_m^3}{3K_r}\left(u\frac{\partial^3 T}{\partial r^3}+w\frac{\partial^3 T}{\partial r^2\partial z}+\frac{u}{r}\frac{\partial^2 T}{\partial r^2}\right)-\frac{16\sigma_0 T_m^3}{3K_r}\left[u\frac{\partial^3 T}{\partial r\partial z^2}+\frac{u}{r^2}\frac{\partial T}{\partial r}\right]-$$
$$\frac{16\sigma_0 T_m^3}{3K_r}\left[w\frac{\partial^3 T}{\partial z^3}+\frac{w}{r}\frac{\partial^2 T}{\partial r\partial z}\right]-\frac{2\sigma_s B_0}{1+\beta_e^2}u\frac{\partial \varphi_e}{\partial r}\frac{\partial w}{\partial r}-\frac{2\sigma_s B_0}{1+\beta_e^2}\left(u\left(w+\frac{k}{R_0}\right)\frac{\partial^2 \varphi_e}{\partial r^2}\right)-$$
$$\frac{2\sigma_s B_0}{1+\beta_e^2}\left(w\left(w+\frac{k}{R_0}\right)\frac{\partial^2 \varphi_e}{\partial r\partial z}+w\frac{\partial \varphi_e}{\partial r}\frac{\partial w}{\partial z}+w\frac{\partial u}{\partial z}\frac{\partial \varphi_e}{\partial z}\right)+\frac{2\sigma_s B_0}{1+\beta_e^2}u^2\frac{\partial^2 \varphi_e}{\partial r\partial z}$$
$$+\frac{2\sigma_s B_0}{1+\beta_e^2}\left(u\frac{\partial u}{\partial r}\frac{\partial \varphi_e}{\partial z}+uw\frac{\partial^2 \varphi_e}{\partial z^2}\right), \tag{33}$$

$$\Sigma_N=u^2\frac{\partial^2 f}{\partial r^2}+2uw\frac{\partial^2 f}{\partial r\partial z}+w^2\frac{\partial^2 f}{\partial z^2}+$$
$$\left(\left(u\frac{\partial u}{\partial r}+w\frac{\partial u}{\partial z}\right)\frac{\partial f}{\partial r}+\left(u\frac{\partial w}{\partial r}+w\frac{\partial w}{\partial z}\right)\frac{\partial f}{\partial z}\right)$$
$$-\frac{D_T}{\vartheta_2}u\left(\frac{\partial^3 T}{\partial r^3}+\frac{1}{r}\frac{\partial^2 T}{\partial r^2}-\frac{1}{r^2}\frac{\partial T}{\partial r}+\frac{\partial^3 T}{\partial r\partial z^2}\right)$$
$$-\frac{D_T}{\vartheta_2}w\left(\frac{\partial^3 T}{\partial z^3}+\frac{1}{r}\frac{\partial^2 T}{\partial r\partial z}+\frac{\partial^3 T}{\partial z\partial r^2}\right). \tag{34}$$

It is compatible to rewrite the preceding governing system of Eqs. (25) - (34) in a suitable non-dimensional format. This can be done in various techniques relying essentially on the choice of the characteristic length, mass, and time. Presume the following non - dimensional forms depending on the characteristic length $=R_0$, the characteristic mass $=\rho_f R_0^3$ and the characteristic time $=R_0^2 k^{-1}$. The

other dimensionless variables are illustrated as follows:

$$u^*=\frac{uR_0}{k\delta_s}, w^*=\frac{wR_0}{k}, z^*=\frac{z}{\lambda_0}, r^*=\frac{r}{R_0}, \delta_s=\frac{R_0}{\lambda_0}, \varepsilon=\frac{a_1}{R_0},$$
$$N_M^*=\frac{N_m R_0^2}{k}, R_e=\frac{\rho_s k}{\mu_{0h}}, P_M^*=\frac{P_m R_0^3}{\lambda_0 k\mu_{0h}}, \tau=\frac{(\rho c)_n}{(\rho c)_s}, v_s=\frac{\mu_{0h}}{\rho_s},$$
$$\beta_A=\frac{K_a}{\mu_{0h}}, T^*=\frac{T-\vartheta_2}{\beta_t R_0}, F=\frac{f-f_0}{f_1^*}, C^*=\frac{C-C_0}{C_1^*}, J_1=\frac{j_m}{R_0^2},$$
$$D_a=\frac{K_p}{R_0^2}, P_r=\frac{\mu_{0h}}{\rho_s k}, R_{cr}=\frac{L_r R_0^2}{k}, E_{ck}=\frac{k^2}{c_s\beta_t R_0^3}, B_r=E_{ck}P_r,$$
$$N_{ip}=\frac{h_p R_0}{D_N}, W_i=\frac{k\varpi}{R_0^2}, \beta_e=\frac{\sigma_0 B_0}{en_e}, \beta_H=\frac{R_G R_0^2}{\mu_{0h}c_s}, \bar{\gamma}_A=\frac{\gamma_a}{\mu_{0h}R_0^2},$$
$$L_M=\frac{v_x}{D}, L_N=\frac{v_s}{D_N}, M_{ic}=\frac{h_c R_0}{D}, \varphi_{E1}^*=\frac{\varphi_e}{E_{f0}R_0}, k=\frac{K_e}{(\rho c)_f},$$
$$\beta_1=\frac{\beta_r}{R_0}, \varphi_E^*=\frac{\varphi_e}{E_f R_0}, z_0^*=\frac{z_0}{\lambda_0}, d_0^*=\frac{d_0}{\lambda_0}, L_0^*=\frac{L_0}{\lambda_0}, R_s^*(z)=\frac{R_s(z)}{R_0},$$
$$\Gamma_H^*=\frac{\lambda_H k}{R_0^2}, \Gamma_N^*=\frac{\lambda_N k}{R_0^2}, E_F^*=\frac{E_{f0}^2 R_0}{kB_0}, L_{e2}^*=e_0\beta_t R_0, H^2=\frac{\sigma_s B_0^2 R_0^2}{\mu_{0h}},$$
$$L_{e1}^*=\frac{\varepsilon_0 E_{f0}^2 R_0^2 (e_0\beta_t R_0)^2}{k\mu_{0h}}, \bar{\xi}=\frac{R_0^2}{k}\xi, R_d=\frac{16\sigma_0 T_m^3}{3K_E K_r}, S_R=\frac{DK_H\beta_t R_0}{kT_m C_1^*},$$
$$D_F=\frac{DK_H C_1^*}{\mu_{0h}c_s C_{ne}\beta_t R_0}, N_B=\frac{\tau D_N f_1^*}{k}, N_T=\frac{\tau D_T\beta_t R_0}{k\vartheta_2},$$
$$H_1^*=\frac{H_1}{R_0}=\varepsilon\cos 2\pi z, s_{rr}=\frac{R_0^2 s_{rr}}{k\mu_{0h}}, s_{rz}=\frac{R_0^2 s_{rz}}{k\mu_{0h}}, s_{zz}=\frac{R_0^2 s_{zz}}{k\mu_{0h}},$$
$$s_{\theta\theta}=\frac{R_0^2 s_{\theta\theta}}{k\mu_{0h}}.$$

(35)

Utilizing the assumption of the long-wavelength approach $(\delta_s << 1)$ with low Reynold's number $(R_e \to 1)$ and substituting by Eq. (35) into Eqs. (25-34), then drooping the star marks for simplicity. Therefore, the governing system of dimensionless differential equations can be expressed as follows:

$$R_e\delta_s^3\left[u\frac{\partial u}{\partial r}+w\frac{\partial u}{\partial z}\right]=\frac{\delta_s}{r}\frac{\partial(rS_{rr})}{\partial r}\delta_s\left[\frac{L_{e1}}{2L_{e2}}\left[\frac{\partial T}{\partial r}\left(\frac{\partial\varphi_E}{\partial r}\right)^2\right]\right]-$$
$$\frac{\delta_s\beta_e H^2}{1+\beta_e^2}\left[E_F\left(\frac{\partial\varphi_E}{\partial r}\right)+(w+1)\right]+\delta_s^2\left(\frac{\partial(S_{rz})}{\partial z}-\frac{1}{D_a}u-\frac{S_{\theta\theta}}{r}\right)$$
$$-\frac{\partial P_M}{\partial r},$$

(36)

$$R_e\delta_s\left[u\frac{\partial w}{\partial r}+w\frac{\partial w}{\partial z}\right]=-\frac{\partial p}{\partial z}-\frac{H^2E_F}{1+\beta_e^2}\left[\frac{\partial\varphi_E}{\partial r}+\beta_e\delta_s\frac{\partial\varphi_E}{\partial z}\right]$$
$$+\frac{H^2}{1+\beta_e^2}\left[\beta_e\delta_s u-(w+1)\right]-\frac{1}{D_a}(w+1)+\frac{1}{r}\frac{\partial(rS_{rz})}{\partial r}+$$
$$\delta\left(\frac{\partial(S_{zz})}{\partial r}+\frac{L_1}{L_2}\frac{\partial T}{\partial z}\left(\frac{\partial\varphi_E}{\partial r}\right)^2\right)+\beta_A\left(\frac{\partial N_M}{\partial r}+\frac{N_M}{r}\right),$$

(37)

$$R_e\delta_s J_1\left[u\frac{\partial N_M}{\partial r}+w\frac{\partial N_M}{\partial z}\right]=-2\beta_A N_M-\beta_A\frac{\partial w}{\partial r}$$
$$+\bar{\gamma}_A\left(\frac{\partial^2 N_M}{\partial r^2}+\frac{1}{r}\frac{\partial N_M}{\partial r}-\frac{N_M}{r^2}\right),$$

(38)

$$(1+R_d)\left[\frac{\partial^2 T}{\partial r^2}+\frac{1}{r}\frac{\partial T}{\partial r}\right]=\delta_s\left(u\frac{\partial T}{\partial r}+w\frac{\partial T}{\partial z}\right)-$$
$$P_r\beta_H T-\frac{H^2B_r}{1+\beta_e^2}(w+1)^2-\frac{H^2B_rE_F^2}{1+\beta_e^2}\left(\frac{\partial\varphi_E}{\partial r}\right)^2$$
$$-\delta_s\Gamma_H[\Pi_E]-\frac{2H^2B_rE_F}{1+\beta_e^2}(w+1)\left(\frac{\partial\varphi_E}{\partial r}\right)-$$
$$\left(D_F P_r\left[\frac{\partial^2 C}{\partial r^2}+\frac{1}{r}\frac{\partial C}{\partial r}\right]+N_B\frac{\partial F}{\partial r}\frac{\partial T}{\partial r}+N_T\left(\frac{\partial T}{\partial r}\right)^2\right),$$

(39)

$$\frac{\partial^2 F}{\partial r^2}+\frac{1}{r}\frac{\partial F}{\partial r}+\frac{N_T}{N_B}\left[\frac{\partial^2 T}{\partial r^2}+\frac{1}{r}\frac{\partial T}{\partial r}\right]=\delta_s u\frac{\partial F}{\partial r}+$$
$$\delta_s w\frac{\partial F}{\partial z}-\delta_s\Gamma_N\frac{N_T}{N_B}w\left(\frac{\partial^3 T}{\partial r^2\partial z}+\frac{1}{r}\frac{\partial^2 T}{\partial r\partial z}\right)$$
$$-\delta_s\Gamma_N\frac{N_T}{N_B}u\left(\frac{\partial^3 T}{\partial r^3}+\frac{1}{r}\frac{\partial^2 T}{\partial r^2}+\frac{1}{r^2}\frac{\partial T}{\partial r}\right),$$

(40)

$$\delta_s L_M\left(u\frac{\partial C}{\partial r}+w\frac{\partial C}{\partial z}\right)=\frac{\partial^2 C}{\partial r^2}+\frac{1}{r}\frac{\partial C}{\partial r}+$$
$$S_R L_M\left[\frac{\partial^2 T}{\partial r^2}+\frac{1}{r}\frac{\partial T}{\partial r}\right]-R_{cr}L_M C,$$

(41)

$$L_{e1}\left[\frac{\partial^2\varphi_E}{\partial r^2}+\frac{1}{r}\frac{\partial\varphi_E}{\partial r}\right]-L_{e2}\,T\left[\frac{\partial^2\varphi_E}{\partial r^2}+\frac{1}{r}\frac{\partial\varphi_E}{\partial r}\right]$$
$$-L_{e2}\frac{\partial T}{\partial r}\frac{\partial\varphi_E}{\partial r}=0,$$

(42)

where,

$$S_{rr}=2\delta_s\left(\left(1-n\right)+nW_i\dot{\bar{\xi}}\right)\frac{\partial u}{\partial r}, \quad (43)$$

$$S_{zz}=2\delta_s\left(\left(1-n\right)+nW_i\dot{\bar{\xi}}\right)\frac{\partial w}{\partial z}, \quad (44)$$

$$S_{\theta\theta}=2\delta_s\left(\left(1-n\right)+nW_i\dot{\bar{\xi}}\right)\frac{u}{r}, \quad (45)$$

$$S_{rz}=\left(\left(1-n\right)+nW_i\dot{\bar{\xi}}\right)\left(\delta_s^2\frac{\partial u}{\partial z}+\frac{\partial w}{\partial r}\right), \quad (46)$$

$$\dot{\bar{\xi}}=\left[2\delta_s^2\left(\frac{\partial u}{\partial r}\right)^2+\left(\delta_s^2\frac{\partial u}{\partial z}+\frac{\partial w}{\partial r}\right)^2+2\delta_s^2\left(\frac{\partial w}{\partial z}\right)^2\right]^{\frac{1}{2}}$$

(47)

$$\Pi_E=N_B\left(u\left(\frac{\partial T}{\partial r}\frac{\partial^2F}{\partial r^2}+\frac{\partial F}{\partial r}\frac{\partial^2T}{\partial r^2}\right)+w\left(\frac{\partial T}{\partial r}\frac{\partial^2F}{\partial r\partial z}+\frac{\partial F}{\partial r}\frac{\partial^2T}{\partial r\partial z}\right)\right)$$
$$+P_r\beta_H\left(u\frac{\partial T}{\partial r}+w\frac{\partial T}{\partial z}\right)+2N_T\left(u\frac{\partial T}{\partial r}\frac{\partial^2T}{\partial r^2}+w\frac{\partial T}{\partial r}\frac{\partial^2T}{\partial r\partial z}\right)+$$
$$D_FP_r\left(u\frac{\partial^3C}{\partial r^3}+w\frac{\partial^3C}{\partial r^2\partial z}+\frac{u}{r}\frac{\partial^2C}{\partial r^2}-\frac{u}{r^2}\frac{\partial C}{\partial r}+\frac{w}{r}\frac{\partial^2C}{\partial r\partial z}\right)+$$
$$R_d\left(u\frac{\partial^3T}{\partial r^3}+w\frac{\partial^3T}{\partial r^2\partial z}+\frac{u}{r}\frac{\partial^2T}{\partial r^2}-\frac{u}{r^2}\frac{\partial T}{\partial r}+\frac{w}{r}\frac{\partial^2T}{\partial r\partial z}\right)+$$
$$\frac{2H^2B_rE_F}{1+\beta_e^2}\left(u(w+1)\frac{\partial^2\varphi_E}{\partial r^2}+u\frac{\partial w}{\partial r}\frac{\partial\varphi_E}{\partial r}+w(w+1)\frac{\partial^2\varphi_E}{\partial r\partial z}\right)$$
$$+\frac{2H^2B_rE_F}{1+\beta_e^2}w\frac{\partial w}{\partial z}\frac{\partial\varphi_E}{\partial r}+\frac{2H^2B_r}{1+\beta_e^2}\left(u(w+1)\frac{\partial w}{\partial r}+w(w+1)\frac{\partial w}{\partial z}\right)$$
$$+\frac{2H^2B_rE_F^2}{1+\beta_e^2}\left(u\frac{\partial\varphi_E}{\partial r}\frac{\partial^2\varphi_E}{\partial r^2}+w\frac{\partial\varphi_E}{\partial r}\frac{\partial^2\varphi_E}{\partial r\partial z}\right).$$

(48)

The convenient boundary conditions may be presented as [3, and 18]:

$$\frac{\partial w}{\partial r}=0, N_M=0, \frac{\partial T}{\partial r}=0, \frac{\partial F}{\partial r}=0, \frac{\partial C}{\partial r}=0,$$
$$\varphi_E=\varphi_{E1}, \quad \text{and} \quad u=0 \quad \text{at} \quad r=r_{s1}, \quad (49)$$

$$w=-1, N_M=0, T+\beta_t\frac{\partial T}{\partial r}=1, \frac{\partial F}{\partial r}+N_{ip}F=0,$$
$$\frac{\partial C}{\partial r}+M_{ic}C=0, \varphi_E=0, \quad u=2\pi\varepsilon\sin 2\pi z$$
$$\text{at} \quad r=r_{s2}=R_s\left(z\right)+H_1 \quad (50)$$

The non- dimensional effective radius of the tube $R_s\left(z\right)$ can be expressed as follows:

$$R_s(z)=\begin{cases}1-m_0\left(z+L_0+d_0\right) & -L_0\le z\le z_0\\ 1-m_0\left(z+L_0+d_0\right)-\dfrac{h_1\cos\omega}{2}\left(1+\cos\left(\dfrac{\pi z}{L_0}\right)\right) & -z_0\le z\le z_0\\ 1-m_0\left(z+L_0+d_0\right) & z_0\le z\le d_0\end{cases} \quad (51)$$

4. Methodology of solution and analysis of convergence:

After using the long wavelength $\left(\delta_s \ll 1\right)$ with low Reynold's number $\left(R_e \ll 1\right)$ supposition. it is recognized that the governing boundary value equations are very tangled to solve analytically. Therefore, we tackle our system of equations (36) – (48) with the appropriate boundary conditions (49) – (50) using a combination between regular perturbation method together with HPM.

4.1. Conventional perturbation method:

By employing the presumption of Verma and Parihar [35], we will presume that the radial velocity u is very teeny when compared with the axial one w. Likewise, the variation in the $z-$ direction is minimal than that in the $r-$ direction. Therefore, one can postulate that $u \ll w$ and $\frac{\partial w}{\partial z} \ll \frac{\partial w}{\partial r}$. Moreover, it follows that the terms $\frac{\partial u}{\partial r}, \frac{\partial u}{\partial z}, \frac{\partial^2 w}{\partial r^2}$ may be disregarded [35]. Over and above, the functions w_0, N_{M0}, T_0, F_0, C_0, and φ_0 will be relied only on r. This case is denoted as the initial state (no peristaltic wave). This takes place only for the system of zero-order of equations (no peristaltic motion). Whilst, in the first – ordered system of equations all terms will be regarded (peristaltic motion).

According to the regular perturbation procedure, we expand our solutions in terms of a small wave number δ_s as follows:

$$\chi = \chi_0 + \delta_s \chi_1 + \delta_s^2 \chi_2 + \cdots\cdots \quad (52)$$

where, χ indicates to any function of the following distributions w, N_M, T, F, C, and φ_E. Also, χ_0 refers to the zero order of δ_s and χ_1 refers to the first order of δ_s.

By substituting from Eq. (52) into the prior system of Eqs. (36) – (48) and collecting the terms of like powers of δ_s produces zero-ordered and first-ordered systems of nonlinear differential equations with the boundary conditions (49) and (50). Due to the complexity in treating these orders, we will make another approximation for these equations by applying homotopy perturbation method. Through the following subsections, we shall introduce these orders.

4.1.1. Zero– order system for δ_s :

$$\frac{\partial P_M}{\partial r} = 0, \quad (53)$$

$$(1-n_h)\left[\frac{\partial^2 w_0}{\partial r^2} + \frac{1}{r}\frac{\partial w_0}{\partial r}\right] - \frac{\partial P_M}{\partial z} - \frac{H^2 E_F}{1+\beta_e^2}\frac{\partial \varphi_{E0}}{\partial r} - \left(\frac{H^2}{1+\beta_e^2} + \frac{1}{D_a}\right)(w_0+1) + \frac{n_h W_i}{r}\frac{\partial}{\partial r}\left(r\left(\frac{\partial w_0}{\partial r}\right)^2\right) + \beta_A\left(\frac{\partial N_{M0}}{\partial r} + \frac{N_{M0}}{r}\right) = 0, \quad (54)$$

$$\overline{\gamma}_A\left(\frac{\partial^2 N_{M0}}{\partial r^2} + \frac{1}{r}\frac{\partial N_{M0}}{\partial r} - \frac{N_{M0}}{r^2}\right) - 2\beta_A N_{M0} - \beta_A \frac{\partial w_0}{\partial r} = 0, \quad (55)$$

$$(1+R_d)\left[\frac{\partial^2 T_0}{\partial r^2} + \frac{1}{r}\frac{\partial T_0}{\partial r}\right] = -P_r \beta_H T_0 - \frac{H^2 B_r}{1+\beta_e^2}(w_0+1)^2 - \frac{H^2 B_r E_F^2}{1+\beta_e^2}\left(\frac{\partial \varphi_{E0}}{\partial r}\right)^2 - \frac{2H^2 B_r E_F}{1+\beta_e^2}(w_0+1)\left(\frac{\partial \varphi_{E0}}{\partial r}\right) - \left(D_u P_r\left[\frac{\partial^2 C_0}{\partial r^2} + \frac{1}{r}\frac{\partial C_0}{\partial r}\right] + N_B \frac{\partial F_0}{\partial r}\frac{\partial T_0}{\partial r} + N_T\left(\frac{\partial T_0}{\partial r}\right)^2\right), \quad (56)$$

$$\frac{\partial^2 F_0}{\partial r^2} + \frac{1}{r}\frac{\partial F_0}{\partial r} = -\frac{N_T}{N_B}\left[\frac{\partial^2 T_0}{\partial r^2} + \frac{1}{r}\frac{\partial T_0}{\partial r}\right] \quad (57)$$

$$\frac{\partial^2 C_0}{\partial r^2} + \frac{1}{r}\frac{\partial C_0}{\partial r} + S_R L_M\left[\frac{\partial^2 T_0}{\partial r^2} + \frac{1}{r}\frac{\partial T_0}{\partial r}\right] - R_{cr} L_M C_0 = 0, \quad (58)$$

$$L_{e1}\left[\frac{\partial^2 \varphi_{E0}}{\partial r^2} + \frac{1}{r}\frac{\partial \varphi_{E0}}{\partial r}\right] - L_{e2} T_0\left[\frac{\partial^2 \varphi_{E0}}{\partial r^2} + \frac{1}{r}\frac{\partial \varphi_{E0}}{\partial r}\right] - L_{e2}\frac{\partial T_0}{\partial r}\frac{\partial \varphi_{E0}}{\partial r} = 0. \quad (59)$$

The non-dimensional boundary conditions may be written as:

$$\frac{\partial w_0}{\partial r} = 0, N_{M0} = 0, \frac{\partial T_0}{\partial r} = 0, \frac{\partial F_0}{\partial r} = 0, \frac{\partial C_0}{\partial r} = 0, \varphi_{E0} = \varphi_{E1}, \text{ and } u_0 = 0 \text{ at } r = r_{s1} \quad (60)$$

$$w_0 = -1, N_{M0} = 0, T_0 + \beta_1 \frac{\partial T_0}{\partial r} = 1, \frac{\partial F_0}{\partial r} + M_{ic} F_0 = 0, \frac{\partial C_0}{\partial r} + N_{ip} C_0 = 0, \text{ and } \varphi_{E0} = 0 \text{ at } r = r_{s2} = R_s(z) + H_1 \quad (61)$$

4.1.2. First – order system for δ_s :

$$\frac{L_{e1}}{2L_{e2}}\left[\frac{\partial T_0}{\partial r}\left(\frac{\partial \varphi_{E0}}{\partial r}\right)^2\right] - \frac{\beta_e E_F H^2}{1+\beta_e^2}\left(\frac{\partial \varphi_{E0}}{\partial r}\right) - \frac{\beta_e H^2}{1+\beta_e^2}(w_0+1) = 0, \quad (62)$$

$$\left(1-n_h\right)\left[\frac{\partial^2 w_1}{\partial r^2}+\frac{1}{r}\frac{\partial w_1}{\partial r}\right]-R_e\left[u_0\frac{\partial w_0}{\partial r}+w_0\frac{\partial w_0}{\partial z}\right]$$
$$-\frac{H^2E_F}{1+\beta_e^2}\left(\frac{\partial\varphi_{E1}}{\partial r}+\beta_e\frac{\partial\varphi_{E0}}{\partial z}\right)-\left(\frac{H^2}{1+\beta_e^2}+\frac{1}{D_a}\right)w_1$$
$$-\frac{\beta_e H^2}{1+\beta_e^2}u_0+\frac{L_{e1}}{L_{e2}}\frac{\partial T_0}{\partial z}\left(\frac{\partial\varphi_{E0}}{\partial r}\right)^2+\beta_A\left(\frac{\partial N_{M1}}{\partial r}+\frac{N_{M1}}{r}\right)+$$
$$2n_hW_i\left[\frac{1}{r}\left(\frac{\partial w_0}{\partial r}\right)\left(\frac{\partial w_1}{\partial r}\right)+\left(\frac{\partial w_0}{\partial r}\right)\left(\frac{\partial^2 w_1}{\partial r^2}\right)+\left(\frac{\partial w_1}{\partial r}\right)\left(\frac{\partial^2 w_0}{\partial r^2}\right)\right], \tag{63}$$

$$\overline{\gamma}_A\left(\frac{\partial^2 N_{M1}}{\partial r^2}+\frac{1}{r}\frac{\partial N_{M1}}{\partial r}-\frac{N_{M1}}{r^2}\right)-2\beta_A N_{M1}$$
$$-R_eJ_1\left[u_0\frac{\partial N_{M0}}{\partial r}+w_0\frac{\partial N_{M0}}{\partial z}\right]-\beta_A\frac{\partial w_1}{\partial r}=0, \tag{64}$$

$$\left(1+R_d\right)\left[\frac{\partial^2 T_1}{\partial r^2}+\frac{1}{r}\frac{\partial T_1}{\partial r}\right]=\left(u_0\frac{\partial T_0}{\partial r}+w_0\frac{\partial T_0}{\partial z}\right)$$
$$-P_r\beta_H T_1-\frac{2H^2B_r}{1+\beta_e^2}w_1\left(w_0+1\right)-\Gamma_H\left[\Pi_E\right]_0$$
$$-\frac{2H^2B_rE_F}{1+\beta_e^2}\left[\left(w_0+1\right)\frac{\partial\varphi_{E1}}{\partial r}+w_1\frac{\partial\varphi_{E0}}{\partial r}\right]$$
$$-\left(N_B\left(\frac{\partial F_0}{\partial r}\frac{\partial T_1}{\partial r}+\frac{\partial F_1}{\partial r}\frac{\partial T_0}{\partial r}\right)+2N_T\left(\frac{\partial T_0}{\partial r}\frac{\partial T_1}{\partial r}\right)\right)$$
$$-\frac{2H^2B_rE_F^2}{1+\beta_e^2}\left(\frac{\partial\varphi_{E0}}{\partial r}\frac{\partial\varphi_{E1}}{\partial r}\right)-D_FP_r\left[\frac{\partial^2 C_1}{\partial r^2}+\frac{1}{r}\frac{\partial C_1}{\partial r}\right], \tag{65}$$

$$\frac{\partial^2 F_1}{\partial r^2}+\frac{1}{r}\frac{\partial F_1}{\partial r}=\left(u_0\frac{\partial F_0}{\partial r}+w_0\frac{\partial F_0}{\partial z}\right)-$$
$$\Gamma_N\frac{N_T}{N_B}\left[u_0\left(\frac{\partial^3 T_0}{\partial r^3}+\frac{1}{r}\frac{\partial^2 T_0}{\partial r^2}+\frac{1}{r^2}\frac{\partial T_0}{\partial r}\right)\right]$$
$$-\Gamma_N\frac{N_T}{N_B}\left[w_0\left(\frac{\partial^3 T_0}{\partial r^2\partial z}+\frac{1}{r}\frac{\partial^2 T_0}{\partial r\partial z}\right)\right]-$$
$$\frac{N_T}{N_B}\left[\frac{\partial^2 T_1}{\partial r^2}+\frac{1}{r}\frac{\partial T_1}{\partial r}\right], \tag{66}$$

$$\frac{\partial^2 C_1}{\partial r^2}+\frac{1}{r}\frac{\partial C_1}{\partial r}-L_M\left(u_0\frac{\partial C_0}{\partial r}+w_0\frac{\partial C_0}{\partial z}\right)+$$
$$S_RL_M\left[\frac{\partial^2 T_1}{\partial r^2}+\frac{1}{r}\frac{\partial T_1}{\partial r}\right]-R_{cr}L_MC_1=0, \tag{67}$$

$$L_{e1}\left[\frac{\partial^2\varphi_{E1}}{\partial r^2}+\frac{1}{r}\frac{\partial\varphi_{E1}}{\partial r}\right]-L_{e2}T_0\left(\frac{\partial^2\varphi_{E1}}{\partial r^2}+\frac{1}{r}\frac{\partial\varphi_{E1}}{\partial r}\right)$$
$$-L_{e2}T_1\left(\frac{\partial^2\varphi_{E0}}{\partial r^2}+\frac{1}{r}\frac{\partial\varphi_{E0}}{\partial r}\right)-L_{e2}\frac{\partial T_0}{\partial r}\frac{\partial\varphi_{E1}}{\partial r}$$
$$-L_{e2}\frac{\partial T_1}{\partial r}\frac{\partial\varphi_{E0}}{\partial r}=0, \tag{68}$$

where,

$$\left[\Pi_E\right]_0=N_B\left(u_0\left(\frac{\partial T_0}{\partial r}\frac{\partial^2 F_0}{\partial r^2}+\frac{\partial F_0}{\partial r}\frac{\partial^2 T_0}{\partial r^2}\right)+w_0\left(\frac{\partial T_0}{\partial r}\frac{\partial^2 F_0}{\partial r\partial z}+\frac{\partial F_0}{\partial r}\frac{\partial^2 T_0}{\partial r\partial z}\right)\right)$$
$$+P_r\beta_H\left(u_0\frac{\partial T_0}{\partial r}+w_0\frac{\partial T_0}{\partial z}\right)+2N_T\left(u_0\frac{\partial T_0}{\partial r}\frac{\partial^2 T_0}{\partial r^2}+w_0\frac{\partial T_0}{\partial r}\frac{\partial^2 T_0}{\partial r\partial z}\right)+$$
$$D_FP_r\left(u_0\frac{\partial^3 C_0}{\partial r^3}+w_0\frac{\partial^3 C_0}{\partial r^2\partial z}+\frac{u_0}{r}\frac{\partial^2 C_0}{\partial r^2}-\frac{u_0}{r^2}\frac{\partial C_0}{\partial r}+\frac{w_0}{r}\frac{\partial^2 C_0}{\partial r\partial z}\right)+$$
$$R_d\left(u_0\frac{\partial^3 T_0}{\partial r^3}+w_0\frac{\partial^3 T_0}{\partial r^2\partial z}+\frac{u_0}{r}\frac{\partial^2 T_0}{\partial r^2}-\frac{u_0}{r^2}\frac{\partial T_0}{\partial r}+\frac{w_0}{r}\frac{\partial^2 T_0}{\partial r\partial z}\right)+$$
$$\frac{2H^2B_rE_F^2}{1+\beta_e^2}\left(u_0\frac{\partial\varphi_{E0}}{\partial r}\frac{\partial^2\varphi_{E0}}{\partial r^2}+w_0\frac{\partial\varphi_{E0}}{\partial r}\frac{\partial^2\varphi_{E0}}{\partial r\partial z}\right)$$
$$+\frac{2H^2B_rE_F}{1+\beta_e^2}\left(u_0\left(w_0+1\right)\frac{\partial^2\varphi_{E0}}{\partial r^2}+u_0\frac{\partial w_0}{\partial r}\frac{\partial\varphi_{E0}}{\partial r}\right)+$$
$$\frac{2H^2B_rE_F}{1+\beta_e^2}\left(w_0\left(w_0+1\right)\frac{\partial^2\varphi_{E0}}{\partial r\partial z}+w_0\frac{\partial w_0}{\partial z}\frac{\partial\varphi_{E0}}{\partial r}\right)+$$
$$\frac{2H^2B_r}{1+\beta_e^2}\left(u_0\left(w_0+1\right)\frac{\partial w_0}{\partial r}+w_0\left(w_0+1\right)\frac{\partial w_0}{\partial z}\right). \tag{69}$$

The non-dimensional boundary conditions may be written as:

$$\frac{\partial w_1}{\partial r}=0, N_{M1}=0, \frac{\partial T_1}{\partial r}=0, \frac{\partial F_1}{\partial r}=0, \frac{\partial C_1}{\partial r}=0,$$
$$\varphi_{E1}=0, \quad \text{and} \quad u_1=0 \qquad \text{at} \quad r=r_1 \tag{70}$$

$$w_1 = 0, N_{M1} = 0, T_1 + \beta_1 \frac{\partial T_1}{\partial r} = 0, \frac{\partial F_1}{\partial r} + M_{ic} F_1 = 0,$$
$$\frac{\partial C_1}{\partial r} + N_{ip} C_1 = 0, \quad \text{and} \quad \varphi_{E1} = 0$$

at $r = r_2 = R_s(z) + H_1$ (71)

4.2. Homotopy perturbation method (HPM):

The HPM is a substantial semi-analytical method is applied for getting an approximate solution of any complicated system of differential equations in diverse domains. It combines between the advantages of the homotopy analysis method as well as the conventional perturbation technique. The HPM is clarified for the first time by He [36]. The homotopy procedure is relying on an artificial small parameter $\mathrm{P}_H \in [0,1]$ denoted as the homotopy parameter. So, this small parameter can be set as a coefficient of any term of the problem. The differential equation become in a simple form when $\mathrm{P}_H = 0$. The case when P_H is boosted and arrives to unity, the equation improves to the coveted formularization. At this stage, the foreseed solution will be oncoming to the desired formula.

In accordance with HPM, we postulate that Eqs. (53)-(59) with the suitable boundary conditions (60) and (61) have the solution which may be expressed as:

$$\Omega_0 = \Omega_{00} + \mathrm{P}_H \ \Omega_{01} + \cdots\cdots\cdots \quad (72)$$

where Ω points to any function of the following distributions w_0, N_{M0}, T_0, F_0, C_0, and φ_{E0}. The linear operators are postulated as follows:

$$\mathrm{L}_1(\mathrm{w}) = \frac{1}{r}\frac{\partial}{\partial r}\left(r\frac{\partial w}{\partial r}\right) - \frac{dP_M}{dz}, \quad (73)$$

$$\mathrm{L}_2(\mathrm{N}_M) = \bar{\gamma}_A\left[\frac{1}{r}\frac{\partial}{\partial r}\left(r\frac{\partial \mathrm{N}_M}{\partial r}\right) - \frac{\mathrm{N}_M}{r^2}\right] - \beta_A, \quad (74)$$

$$\mathrm{L}_3(\mathrm{T}) = (1+R_d)\left[\frac{1}{r}\frac{\partial}{\partial r}\left(r\frac{\partial T}{\partial r}\right)\right] - \beta_H, \quad (75)$$

$$\mathrm{L}_4(\mathrm{F}) = \frac{1}{r}\frac{\partial}{\partial r}\left(r\frac{\partial F}{\partial r}\right) + \frac{N_T}{N_B}, \quad (76)$$

$$\mathrm{L}_5(\mathrm{C}) = \frac{1}{r}\frac{\partial}{\partial r}\left(r\frac{\partial C}{\partial r}\right) + S_R L_M, \quad (77)$$

$$\mathrm{L}_6(\varphi_E) = \mathrm{L}_{e1}\left[\frac{1}{r}\frac{\partial}{\partial r}\left(r\frac{\partial \varphi_E}{\partial r}\right)\right] - \mathrm{L}_{e2}. \quad (78)$$

Therefore, the initial guesses solutions can be presumed as follows:

$$w_{00} = -\frac{dP_M}{dz}\left(\frac{1}{4(n_h - 1)}\right) + R_1 \ \mathrm{lnr} + \mathrm{R}_2 \ , \quad (79)$$

$$N_{M00} = \frac{\beta_A}{3\bar{\gamma}_A}\mathrm{r}^2 + \mathrm{R}_3 \ \mathrm{lnr} + \mathrm{R}_4 \ , \quad (80)$$

$$T_{00} = \frac{\beta_H}{4(1+R_d)}\mathrm{r}^2 + \mathrm{R}_5 \ \mathrm{lnr} + \mathrm{R}_6 \ , \quad (81)$$

$$F_{00} = -\frac{1}{4}\frac{N_T}{N_B}r^2 + \mathrm{R}_7 \ \mathrm{lnr} + \mathrm{R}_8 \ , \quad (82)$$

$$C_{00} = -\frac{1}{4}S_R L_M \ r^2 + \mathrm{R}_9 \ \mathrm{lnr} + \mathrm{R}_{10} \ , \quad (83)$$

$$\varphi_{E00} = \frac{1}{4}\frac{L_{e2}}{L_{e1}}r^2 + \mathrm{R}_{11} \ \mathrm{lnr} + \mathrm{R}_{12} \ . \quad (84)$$

As before the first order system is also very intricated to solve it. Thus, we will apply the HPM again for solving this system. According to HPM, we presume that Eqs. (62) - (69) with the convenient boundary conditions (70) and (71) have the solution of the formula:

$$\alpha_1 = \alpha_{10} + \mathrm{P}_H \ \alpha_{11} + \cdots\cdots\cdots, \quad (85)$$

where α indicates to any function of the following distributions: w_1, N_{M1}, T_1, F_1, C_1, and φ_{E1}.

By regarding the same preceding steps and applying HPM as well as the linear operators' definitions, the initial guesses solutions may be presupposed as follows:

$$w_{10} = R_{25} \ \mathrm{lnr} + \mathrm{R}_{26} \ , \quad (86)$$

$$N_{M10} = \mathrm{R}_{27}\ \ln r + \mathrm{R}_{28}\ ,$$
(87)

$$T_{10} = \mathrm{R}_{29}\ \ln r + \mathrm{R}_{30}\ ,$$
(88)

$$F_{10} = \mathrm{R}_{31}\ \ln r + \mathrm{R}_{32}\ ,$$
(89)

$$C_{10} = \mathrm{R}_{33}\ \ln r + \mathrm{R}_{34}\ ,$$
(90)

$$\varphi_{E10} = \mathrm{R}_{35}\ \ln r + \mathrm{R}_{36}\ ,$$
(91)

On employing the preceding power series solution into Eqs. (53)-(59) with (60) and (61) in addition (62)-(69) with (70) and (71), then equate the coefficients of like powers of P_H on all of them. At the end, solve the resultant linear system of equations. One gets the semi-analytic solutions of the various stages of P_H^n. The entire solution is gained by setting $P_H = 1$. The solutions are calculated up to the first order. Thus, all complete solutions for the former distributions in terms of δ_s may be expressed as follows:

$$\mathrm{w} = -\frac{1}{4(\mathrm{n_h}-1)}\frac{\mathrm{dP_M}}{\mathrm{dz}}\mathrm{r}^2 + (\mathrm{R}_1+\mathrm{R}_{13})\ln r + (\mathrm{R}_2+\mathrm{R}_{14}) + N_1 r + \frac{N_2}{\mathrm{r}} + N_3\mathrm{r}^3 + N_4\mathrm{r}^4 +$$

$$\delta\left(\begin{array}{l}
(\mathrm{R}_{25}+\mathrm{R}_{37})\ln r + (\mathrm{R}_{26}+\mathrm{R}_{38}) + N_5 r + N_6\mathrm{r}^2 + N_7\mathrm{r}^3 + N_8\mathrm{r}^4 \\
+N_9\mathrm{r}^5 + N_{10}\mathrm{r}^6 + N_{11}\mathrm{r}^7 + N_{12}\mathrm{r}^8 + N_{13}\mathrm{r}^9 + N_{14}\mathrm{r}^{10} + N_{15}\mathrm{r}^{11} \\
+N_{16}\mathrm{r}^{12} + N_{18}\mathrm{r}^{13} + N_{19}\mathrm{r}^{14} + N_{20}\mathrm{r}^2\ln r + N_{21}\mathrm{r}^3\ln r + \\
N_{22}\mathrm{r}^4\ln r + N_{23}\mathrm{r}^5\ln r + N_{24}\mathrm{r}^6\ln r + N_{25}\mathrm{r}^7\ln r + N_{26}\mathrm{r}^8\ln r \\
+N_{27}\mathrm{r}^9\ln r + N_{28}\mathrm{r}^{10}\ln r + N_{29}\mathrm{r}^2(\ln r)^2 + N_{30}\mathrm{r}^3(\ln r)^2 + \\
N_{31}\mathrm{r}^4(\ln r)^2 + N_{32}\mathrm{r}^5(\ln r)^2 + N_{33}\mathrm{r}^6(\ln r)^2 + N_{34}\mathrm{r}^7(\ln r)^2 \\
+N_{35}\mathrm{r}^8(\ln r)^2 + N_{36}\mathrm{r}^9(\ln r)^2 + N_{37}\mathrm{r}^{10}(\ln r)^2 + N_{38}(\ln r)^2 \\
+N_{39}\mathrm{r}^2(\ln r)^3 + N_{40}\mathrm{r}^3(\ln r)^3 + N_{41}\mathrm{r}^4(\ln r)^3 + N_{42}\mathrm{r}^5(\ln r)^3 \\
+N_{43}\mathrm{r}^6(\ln r)^3 + N_{44}\mathrm{r}^7(\ln r)^3 + N_{45}\mathrm{r}^2(\ln r)^4 + N_{46}\mathrm{r}^3(\ln r)^4 \\
+N_{47}\mathrm{r}^4(\ln r)^4 + N_{48}\mathrm{r}^5(\ln r)^4 + N_{49}\mathrm{r}^6(\ln r)^4 + N_{50}\mathrm{r}^2(\ln r)^5 \\
+N_{51}\mathrm{r}^3(\ln r)^5 + N_{52}\mathrm{r}^4(\ln r)^5
\end{array}\right),$$
(92)

$$N_M = \frac{1}{3}\frac{\beta_{\mathrm{A}}}{\gamma_A}\mathrm{r}^2 + (\mathrm{R}_3+\mathrm{R}_{15})r^{-1} + (\mathrm{R}_4+\mathrm{R}_{16})r + N_{53}r + N_{54}\mathrm{r}^3 + N_{55}\mathrm{r}^4 + N_{65}r\ln r +$$

$$\delta\left(\begin{array}{l}
(\mathrm{R}_{27}+\mathrm{R}_{39})r^{-1} + (\mathrm{R}_{28}+\mathrm{R}_{40})r + N_{57}r + N_{58}\mathrm{r}^2 + \\
N_{59}\mathrm{r}^3 + N_{60}\mathrm{r}^4 + N_{61}\mathrm{r}^5 + N_{62}\mathrm{r}^6 + N_{63}\mathrm{r}^7 + N_{64}\mathrm{r}^8 \\
+N_{65}\mathrm{r}^9 + N_{66}\mathrm{r}\ln r + N_{67}\mathrm{r}^2\ln r + N_{68}\mathrm{r}^3\ln r + \\
N_{69}\mathrm{r}^4\ln r + N_{70}\mathrm{r}^5\ln r + N_{71}\mathrm{r}^6\ln r + N_{72}\mathrm{r}^7\ln r + \\
N_{73}\mathrm{r}(\ln r)^2 + N_{74}\mathrm{r}^3(\ln r)^2 + N_{75}\mathrm{r}^5(\ln r)^2 + N_{76}
\end{array}\right),$$
(93)

$$T = \frac{\beta_{\mathrm{H}}}{4(1+\mathrm{R_d})}\mathrm{r}^2 + (\mathrm{R}_5+\mathrm{R}_{17})\ln r + (\mathrm{R}_6+\mathrm{R}_{18}) + N_{77}r + N_{78}\mathrm{r}^2 + N_{79}\mathrm{r}^3 + N_{80}\mathrm{r}^4 + N_{81}\mathrm{r}^5 + N_{82}\mathrm{r}^6 + N_{83}r\ln r +$$

$$N_{84}\mathrm{r}^2\ln r + N_{85}\mathrm{r}^3\ln r + N_{86}\mathrm{r}^4\ln r + N_{87}\mathrm{r}^2(\ln r)^2 + N_{88}(\ln r)^2 +$$

$$\delta\left(\begin{array}{l}
(\mathrm{R}_{29}+\mathrm{R}_{41})\ln r + (\mathrm{R}_{30}+\mathrm{R}_{42}) + N_{89}r + N_{90}\mathrm{r}^2 + N_{91}\mathrm{r}^3 + \\
N_{92}\mathrm{r}^4 + N_{93}\mathrm{r}^5 + N_{94}\mathrm{r}^6 + N_{95}\mathrm{r}^7 + N_{96}\mathrm{r}^8 + N_{97}\mathrm{r}^9 + N_{98}\mathrm{r}^{10} \\
+N_{99}\mathrm{r}^{11} + N_{100}\mathrm{r}^{12} + N_{101}\mathrm{r}^{13} + N_{102}\mathrm{r}^{14} + N_{103}r^{-1}\ln r + N_{104}r\ln r \\
+N_{105}\mathrm{r}^2\ln r + N_{106}\mathrm{r}^3\ln r + N_{107}\mathrm{r}^4\ln r + N_{108}\mathrm{r}^5\ln r + N_{109}\mathrm{r}^6\ln r \\
+N_{110}\mathrm{r}^7\ln r + N_{111}\mathrm{r}^8\ln r + N_{112}\mathrm{r}^9\ln r + N_{113}\mathrm{r}^{10}\ln r + N_{114}\mathrm{r}^{11}\ln r \\
+N_{115}\mathrm{r}^{12}\ln r + N_{116}\mathrm{r}(\ln r)^2 + N_{117}\mathrm{r}^2(\ln r)^2 + N_{118}\mathrm{r}^3(\ln r)^2 + \\
N_{119}\mathrm{r}^4(\ln r)^2 + N_{120}\mathrm{r}^5(\ln r)^2 + N_{121}\mathrm{r}^6(\ln r)^2 + N_{122}\mathrm{r}^7(\ln r)^2 + \\
N_{123}\mathrm{r}^8(\ln r)^2 + N_{124}\mathrm{r}^9(\ln r)^2 + N_{125}\mathrm{r}^{10}(\ln r)^2 + N_{126}(\ln r)^2 + \\
N_{127}\mathrm{r}(\ln r)^3 + N_{128}\mathrm{r}^2(\ln r)^3 + N_{129}\mathrm{r}^3(\ln r)^3 + N_{130}\mathrm{r}^4(\ln r)^3 + \\
N_{131}\mathrm{r}^5(\ln r)^3 + N_{132}\mathrm{r}^6(\ln r)^3 + N_{133}\mathrm{r}^7(\ln r)^3 + N_{134}\mathrm{r}^8(\ln r)^3 + \\
N_{135}(\ln r)^3 + N_{136}\mathrm{r}^3(\ln r)^4 + N_{137}\mathrm{r}^4(\ln r)^4 + N_{138}\mathrm{r}^5(\ln r)^4 + \\
N_{139}\mathrm{r}^6(\ln r)^4 + N_{140}(\ln r)^4 + N_{141}\mathrm{r}^4(\ln r)^5 \\
+N_{142}\mathrm{r}^4(\ln r)^5 + N_{143}(\ln r)^5
\end{array}\right),$$
(94)

$$F = -\frac{1}{4}\frac{\mathrm{N_T}}{\mathrm{N_B}}\mathrm{r}^2+\left(\mathrm{R}_7+\mathrm{R}_{19}\right)\ln r+\left(\mathrm{R}_8+\mathrm{R}_{20}\right)+$$
$$\delta\begin{pmatrix}\left(\mathrm{R}_{31}+\mathrm{R}_{43}\right)\ln r+\left(\mathrm{R}_{32}+\mathrm{R}_{44}\right)+N_{144}r+\\ N_{145}\mathrm{r}^2+N_{146}\mathrm{r}^3+N_{147}\mathrm{r}^4+N_{148}\mathrm{r}^5+N_{149}\mathrm{r}^6+\\ N_{150}\mathrm{r}^7+N_{151}\mathrm{r}^8+N_{152}r\ln r+N_{153}\mathrm{r}^2\ln r+\\ N_{154}\mathrm{r}^3\ln r+N_{155}\mathrm{r}^4\ln r+N_{156}\mathrm{r}\left(\ln r\right)^2+\\ N_{157}\mathrm{r}^2\left(\ln r\right)^2+N_{158}\mathrm{r}^3\left(\ln r\right)^2+N_{160}\mathrm{r}^4\left(\ln r\right)^2\\ +N_{161}\left(\ln r\right)^2+N_{162}\left(\ln r\right)^3\end{pmatrix},$$

(95)

$$C = -\frac{1}{4}\mathrm{S_R L_M r}^2+\left(\mathrm{R}_9+\mathrm{R}_{21}\right)\ln r+\left(\mathrm{R}_{10}+\mathrm{R}_{22}\right)$$
$$+N_{163}\mathrm{r}^2+N_{164}\mathrm{r}^4+N_{165}\mathrm{r}^2\ln r+$$
$$\delta\begin{pmatrix}\left(\mathrm{R}_{33}+\mathrm{R}_{45}\right)\ln r+\left(\mathrm{R}_{34}+\mathrm{R}_{46}\right)+N_{166}r+\\ N_{167}\mathrm{r}^2+N_{168}\mathrm{r}^3+N_{169}\mathrm{r}^4+N_{170}\mathrm{r}^5+N_{171}\mathrm{r}^6\\ +N_{172}\mathrm{r}^7+N_{173}\mathrm{r}^8+N_{174}\mathrm{r}^9+N_{175}r\ln r+\\ N_{176}\mathrm{r}^2\ln r+N_{177}\mathrm{r}^3\ln r+N_{178}\mathrm{r}^4\ln r+\\ N_{179}\mathrm{r}^5\ln r+N_{180}\mathrm{r}^6\ln r+N_{181}\mathrm{r}^7\ln r+\\ N_{182}\mathrm{r}^2\left(\ln r\right)^2+N_{183}\mathrm{r}^3\left(\ln r\right)^2+N_{184}\mathrm{r}^4\left(\ln r\right)^2\\ +N_{185}\mathrm{r}^5\left(\ln r\right)^2\end{pmatrix},$$

(96)

$$\varphi_E = \frac{1}{4}\frac{L_{\mathrm{e2}}}{L_{\mathrm{e1}}}\mathrm{r}^2+\left(\mathrm{R}_{11}+\mathrm{R}_{23}\right)\ln r+\left(\mathrm{R}_{12}+\mathrm{R}_{24}\right)$$
$$+N_{186}r+N_{187}\mathrm{r}^2+N_{188}\mathrm{r}^3+N_{189}\mathrm{r}^4+N_{190}\mathrm{r}^2\ln r+$$
$$N_{191}\left(\ln r\right)^2+N_{192}+\delta\left(\left(\mathrm{R}_{35}+\mathrm{R}_{47}\right)\ln r+\left(\mathrm{R}_{36}+\mathrm{R}_{48}\right)\right),$$

(97)

where, the arbitrary constants $\left(R_1-R_{48}\right)$ and the coefficients $\left(N_1-N_{192}\right)$ that appeared in the above equations from (92) to (97) are not included in the manuscript to save the length. They are obtainable under the request of the referees.

As a special case of our analytical study, in the absence of nanoparticles concertation, spin velocity, electric potential, mild stenosis, and chemical reaction. On the other hand, when we set the parameters

$$\begin{pmatrix}R_{\mathrm{d}}=0,\ W_{\mathrm{i}}=0,\ N_T=0,\ L_{e1}=0,\ D_a\to\infty,h=0,\\ \beta_H=0,H=0,\ \beta_e=0,\ \bar{\gamma}_A=0,\ \beta_A=0,R_{cr}=0,\end{pmatrix}$$

and $\Gamma_N=0$, one can return to the work of Hayat et al. [12]

5. Numerical results and discussions

By employing the Mathematica software to display the impacts of the varied physical variables which encompassed in our analytic investigation on the resultant distributions. the utilized ranges of the assorted parameters are presenting in diverse works apropos our study [3, 11, 29, and 30]. These ranges may be expressed as

$$(P_r=2.0,\ \varepsilon=0.02,\ H=3,\ z=0.2,$$
$$N_B=0.5,\ S_R=0.5,\ L_M=0.3,\ \bar{\gamma}_A=0.5,$$
$$\beta_H=0.5,\ L_N=0.5,\ N_{ip}=0.4,\ N_{ic}=0.4,$$
$$D_a=0.02,\ a_0=0.2,\ z_0=0.2,\ n_h=1.5,$$
$$\delta=0.1,\ R_e=0.1,\ R_{cr}=0.1,\ h=0.1,$$
$$\beta_t=0.5,\ E_F=0.6,\ B_r=0.3,\ L_0=1,$$
$$\beta_e=0.2,\ d_0=1,\ L_{e1}=0.2,\ D_f=1,$$
$$R_{cr}=0.5,\ \omega=0.05,\ \beta_A=0.5,\ L_{e2}=0.1,$$
$$\Gamma_H=1.5,\ \Gamma_N=1.5,\text{ and }\ N_T=0.5).$$

The impact of the electrical Rayleigh number L_{e1} on the axial velocity $w(r)$ is indicated throughout Fig. 2. It is evident that the velocity enriches with the elevation in L_{e1} along the interval $r\in[0.1,0.4]$. Whilst, the opposite happens along the interval $r\in[0.42,0.8]$. Fig 3 exposes the variation of $w(r)$ for various magnitudes of Hartman number H. It is recognized that $w(r)$ declines with an elevation in H. In reality, Hartman number H is denoted as the ratio amidst the magnetic force and the viscous one. In addition, it deemed as a dimensionless number that gives a measure of the relative significance of drag forces resulting from magnetic induction and viscous forces in Hartmann influx and determines the velocity profile for such influx. Thus, it is observed that the larger magnitudes of H lead to decay in $w(r)$. Physiologically, this phenomenon is complying with the theory which explain that rising in H is responsible for improving in Lorentz force which impedes the fluid influx motion. This reveals that if we enlarge the strength of H, the influx will

be encumbered. This important resultant conduct has an essential role in industrial applications, particularly in favours to solidification processes as casting and semiconductor single crystal growth applications. Also, the employing of magnetic particles in the recuperation of cancer is less focused on the delivery of drugs and more on their utilize as a new therapeutic outset in which tumour cells are stained by applying local heat through an external magnetic field. This observation is in a great complying with those attained by [2, 3, 11, 15, 19 and 30]. The influence of D_a on $w(r)$ is introduced through Fig.4. it is noticed that $w(r)$ escalates with an enrichment in D_a . In fact, Darcy number is defined as the capacity of the porosity of the medium. Rising the porosity of the permeable porous medium leads to a dwindling in the resistance to the fluid. Thus, greater values of the medium porosity need more space to influx as a consequence its velocity increases. This conduct is in a good congruent with this obtained by [2].

Fig. 5 exhibits the variance of $w(r)$ for different values of E_F. It is obvious that $w(r)$ dwindles with the escalating in E_F. In reality, electromagnetic interactions in the influx are responsible of this reduction demeanour. The influence of taper angle ω on $w(r)$ is portrays though Fig.6. In fact, the influence of vessel tapering in the existence of the stenosis merit specific attention due to its extreme importance. Additionally, the tapering has a substantial considerable role in the arterial system [35]. Consequently, this present study focused on discussing the influx inside a tapered tube in the existence of the stenosis. It is indicated that in case of the diverging tapered $\omega = 0.10, 0.05, (\omega > 0)$, the magnitude of the axial velocity $w(r)$ is larger than the other both cases (the non-tapered artery $\omega = 0$ and the convergent tapered $\omega = -0.05, (\omega < 0)$). Also, it is obvious that the axial velocity is elevated with the escalating in ω. Fig. 7 shows the impact of β_e on $w(r)$. It is depicting that β_e has an improving impact on $w(r)$. Actually, greater values of β_e caused the effective conductivity to be dwindled. That leads to a declination in the force of magnetic damping. Thus, the axial velocity $w(r)$ promotes. These impacts are fully complying with [3,19, 29 and 30].

The variation of $N_M(r)$ for diverse magnitudes of $\overline{\gamma}_A$ is depicted through Fig. 8. It is recognized that $N_M(r)$ is always positive and declined with the enhancement of $\overline{\gamma}_A$. This observed result is congruent with the work of [3, and 5]. Fig. 9 explains the demeanour of β_A on $N_M(r)$. It is obvious that $N_M(r)$ is always positive and enhances with the elevation in β_A. This noticed outcome is fully complying with this reported by [3, and 5].

Fig. 10 presents the influences of Γ_H on $T(r)$. As noticed from this figure, $T(r)$ declines with the elevation in Γ_H. In a view of the physiological situation, the enrich in Γ_H causes a non-conducting demeanour. Furthermore, it is noticed that the particles take more time to transport heat to its adjoining particles, which leads to decline in $T(r)$. Over and above, $T(r)$ elevates only in the absence of Γ_H i.e., $(\Gamma_H = 0)$. Consequently, $T(r)$ is lower in the case of Cattaneo-Christov heat flux model when compared to classical Fourier's law. This obtained outcome is complying with those displayed by [11, 13, 14, and 15]. The impact of R_d on $T(r)$ is exposed through Fig. 11. It is recognized that $T(r)$ deemed as a reduction function with the increment in R_d. Actually, this reduction conduct is caused due to pervasion of the molecular energy of the fluid, that responsible for making R_d behave like that. This obtained outcome is fully agreement with the outcome reported by [2, 5, 19, and 34].

The influence of the thermophoretic parameter N_T on $F(r)$ is examined through Fig. 12. As shown from that figure, the elevation in N_T lead to an enrichment in $F(r)$. From the physiological point of view, elevating the thermophoretic parameter

N_T creates the larger mass influx due to temperature gradient which in turn enhances the concentration. This noticed outcome is fully consistent with this displayed by [2, 3, 11, and 15]. Fig. 13 exhibits the variation of $F(r)$ for several values of nano Biot number N_{ip}. It is found that $F(r)$ dwindled with the increment in N_{ip}. In the physical visualization, this conduct occurs since larger values of N_{ip} lead nanoparticles to need more time to diffuse that shows dwindling in $F(r)$. This resultant observation is fully agreement with the work of [3].

The variance of the concentration $C(r)$ for varied values of the chemical reaction parameter R_{cr} is scrutinized through Fig. 14. It is indicated that the concentration $C(r)$ is always negative and dwindled with the augmenting in R_{cr}. The physical justification, chemical reaction parameter R_{cr} consolidates the rate of the interfacial mass transfer that leads to dwindle in the concentration profile $C(r)$. This resultant demeanour is fully consistent to those displayed by [29]. Fig. 15 explains the impact of the Lewis number L_M on the concentration $C(r)$. It is evident that the concentration $C(r)$ declines with an elevation in L_M. Physiologically, the Lewis number L_M is known as the ratio amidst the thermal diffusivity to mass diffusivity (or) "Schmidt number to Prandtl number". This is employed to characterize flows in which there is simultaneous heat and mass (by convection) transfer. Thus, the enrich in L_M causes the mass diffusion to decay that gives elevate in the inter-molecular force and causes a decline in fluid concentration $C(r)$. The examining of Lewis number is significant to characterize fluid influx where there is heat and mass transfer. As well, there is a reverse proportion amidst the Lewis number L_M and the Prandtl number P_r. This obtained demeanour is fully congruent to the results displayed by [3, 11, and 15].

Fig.16 describes the influence of the electrical Rayleigh number L_{e1} on the electric potential $\varphi_E(r)$. Hither, the alternating current (Ac) of electric field is employed in order to create a dipole charge that conserve on the shape of the peristaltic waves. It is noticed that the electric potential $\varphi_E(r)$ enlarges by the elevate of L_{e1}. The impact of the adverse temperature parameter L_{e2} on the electric potential $\varphi_E(r)$ is displayed through Fig.17. As shown in this figure, the electric potential $\varphi_E(r)$ declines with an enhancement in L_{e2}. These significant outcomes are complying to those reported by [29].

Fig. (2)

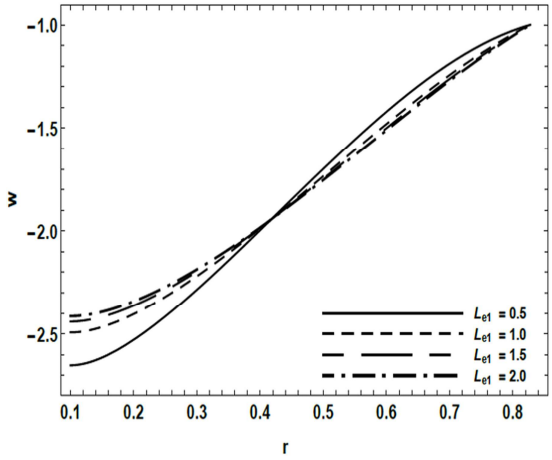

Fig. (3)

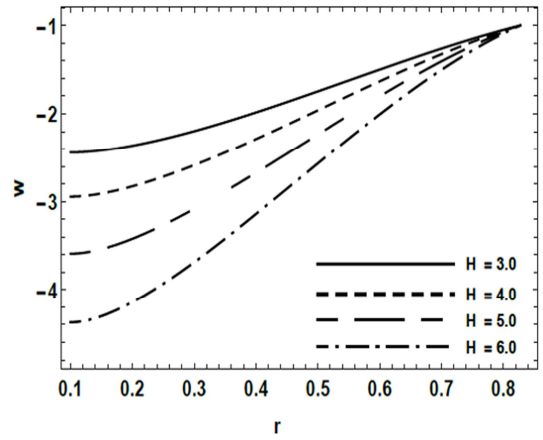

Fig. (4)

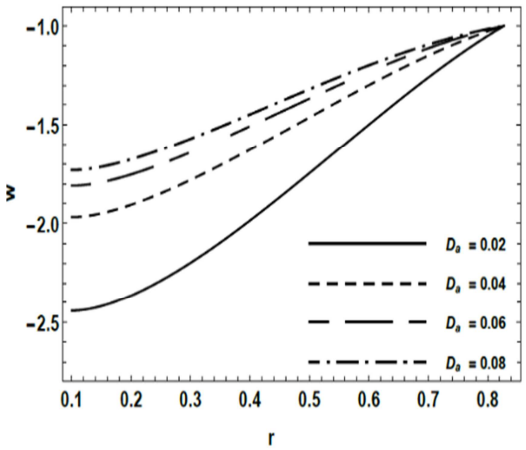

Fig. (5)

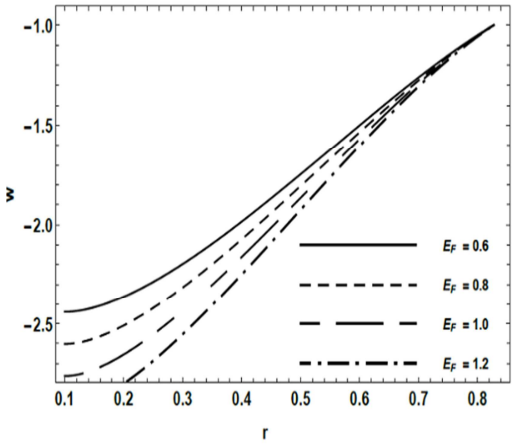

Fig. (6)

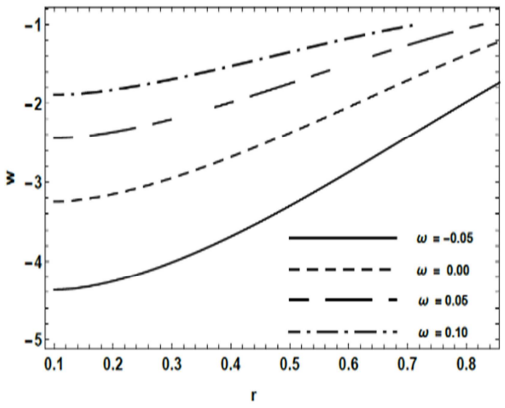

Fig. (7)

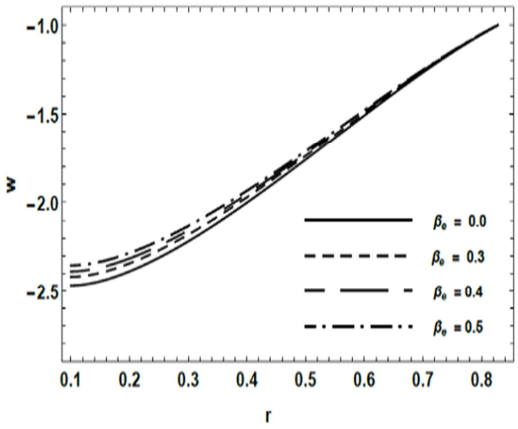

Fig. (8)

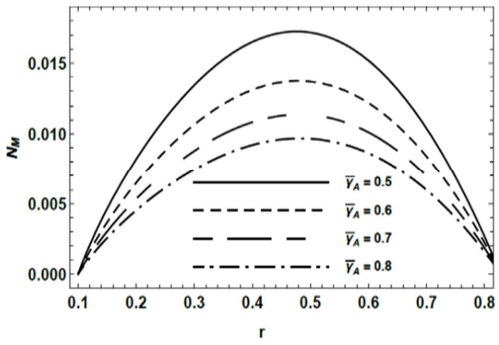

Fig. (9)

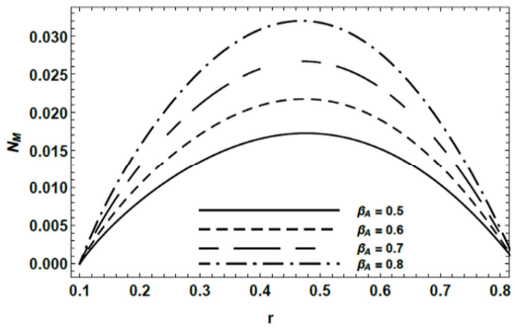

Fig. (10)

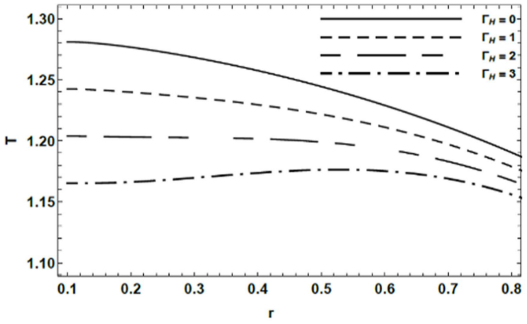

Fig. (11)

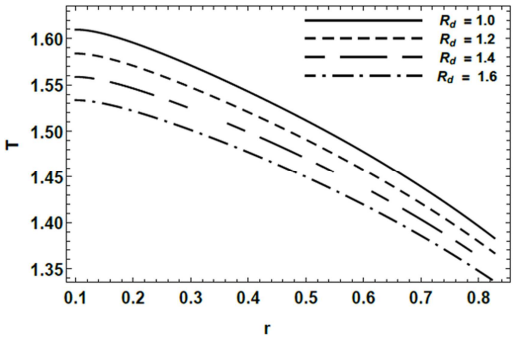

Fig. (12)

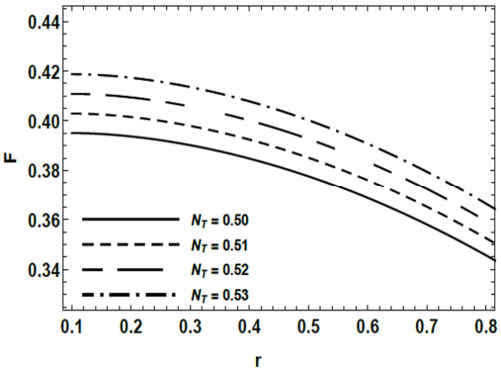

Fig. (13)

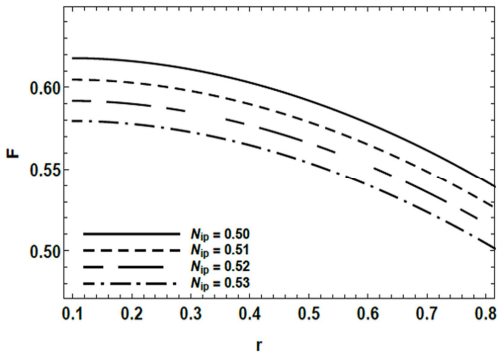

Fig. (14)

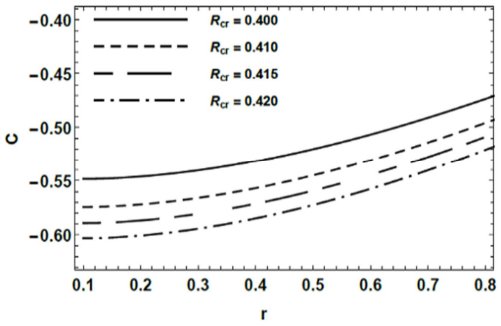

Fig. (15)

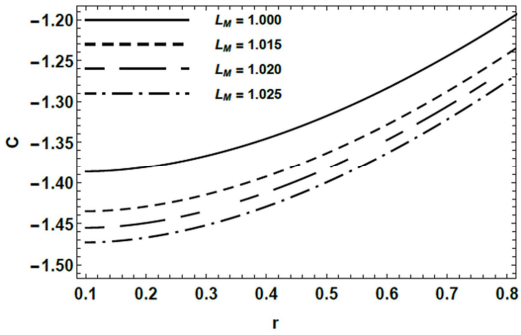

Fig. (16)

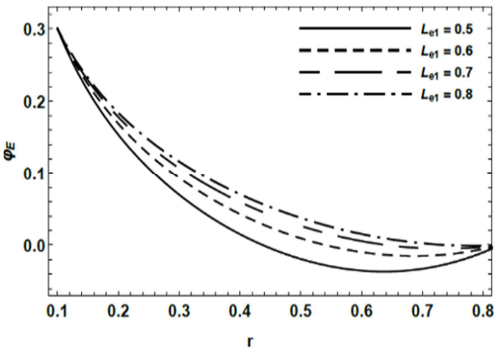

Fig. (17)

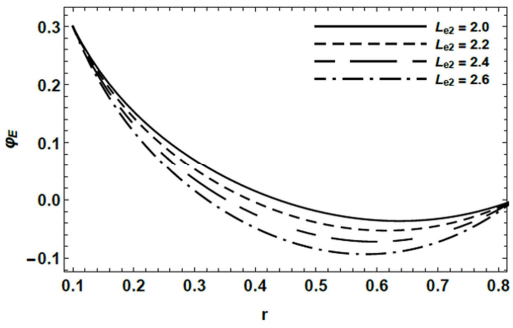

6. Conclusion

The notion of the current analytical study is to exhibit the impact of Cattaneo-Christov double

diffusion on peristaltic flow of tangent hyperbolic micropolar nanofluid inside an artery in the existence of mild stenosis. The effects of Hall currents, thermal radiation, ohmic dissipation, Soret, Dufour, heat generation and chemical reaction are also imposed. Furthermore, the convective conditions for both distributions of concentration as well as nano phenomenon and slip condition for temperature distribution are presumed. It is found that, the axial velocity $w(r)$ decreases with the elevation in both H, E_F. Whilst, it **enhances** with the enlarging in D_a, ω, β_e. The electrical Rayleigh number L_{e1} has a dual impact on the axial velocity $w(r)$. Further, the spin velocity $N_M(r)$ declines with an elevation in $\overline{\gamma}_A$. Meanwhile, enlarging in β_A leads to escalate $N_M(r)$. Moreover, the temperature $T(r)$ decays with an enhancement in both Γ_H, R_d. Furthermore, the elevating in N_T causes an increment in the nanoparticles concentration $F(r)$. Whereas, it declines with rising in N_{ip}. The concentration $C(r)$ dwindled with an escalating in both R_{cr}, L_M. Finally, the electric potential $\varphi_E(r)$ diminishes with an enlargement in L_{e1}. Whilst, elevating in L_{e2} causes rising in $\varphi_E(r)$. The foregoing outcomes may have applied in diverse scientific fields, which interested in discussing in the peristaltic transfer of non-Newtonian micropolar nanofluids flow through stenosed artery with Cattaneo-Christov double diffusion analytically. Further, this analysis study has various applications in diverse areas as, medicine, medical-industrial, and several other implementations. Through the physiological perspective, our model relates to sinusoidal waves that happen in the intestines, oesophagus, and stomach. In addition, the current consideration is very substantial in a significant medical implementation like endoscope, The endoscope has several clinical applications. Hence, it is considered to be a very significant tool utilized in determining real reasons responsible for many problems [37-64]. Moreover, in the human organs in which fluid is transported by peristaltic pumping, such as the stomach, small intestine, etc. Consequently, the present study introduces a description demonstrate the peristaltic motion of blood flow through a stenosed artery.

Nomenclature

$\underline{A}_1 h$	The first Rivilin Ericksen tensor
a_1	Wave amplitude
B_0	Magnetic field strength
B_r	Brinkman number
c_e	Speed of wave
c_s	Specific heat parameter of fluid
c_n	Specific heat of nanoparticle
C_{en}	Concentration susceptibility
C	Dimensionless concentration
R	Half-channel width
D	Coefficient of mass diffusivity
D_a	Darcy number
D_N	Brownian diffusion coefficient
D_T	Thermophoretic coefficient
D_F	Dufour number
e_0	Thermal expansion coefficient of dielectric constant
E_{ck}	Eckert number
E_F	Electromagnetic parameter
E_r	Electric field
h	Maximum height of stenosis
H	Height of stenosis in tapered artery
H	Hartman number
h_c	Mass transfer coefficient
h_p	Nanofluid coefficient
$\underline{J}_1$	Current density
J_A	Microinertia constant
k	Thermophoretic conductivity
K	Permeability of porous medium
K_E	Thermal conductivity
K_r	Rosseland absorption coefficient
K_H	Thermal diffusion ratio
L_{e1}	Electrical Rayleigh number
L_{e2}	Temperature parameter
L_r	Constant of chemical reaction
L_M	Lewis number
L_N	Nano Lewis number
m_0	Slope of tapered vessel
M_{ic}	Mass transfer Biot number

n_h	The power law index
N_B	Brownian motion parameter
N_T	Thermophoresis parameter
N_{ip}	Nano Biot number
P_M	Modified fluid pressure
P_r	Prandtl number
$R_s^*(z)$	Radius of tapered artery
R_0	Radius of un tapered artery
R_G	Constant of heat addition and absorption.
R_{cr}	Non-dimension chemical reaction parameter
R_e	Reynold's number
S_R	Soret number
t	Time
T	Dimensionless fluid temperature
T_m	Mean fluid temperature
W_i	Weissenberg number
z_0	Half-length of stenosis
	Greek symbols
β_1	Thermal slip parameter
β_A	Micropolar dimensionless viscosity
β_e	Hall parameter
β_H	Mean absorption coefficient
β_t	adverse temperature gradient
Γ_H	Thermal relaxation time
Γ_N	Nano relaxation time
φ_e	Electric potential
ϑ_1	Temperature of the lower wall
ϑ_2	Temperature of the upper wall
ρ_e	Free charge density
δ_s	Wave number
γ_a	Spin-gradient viscosity
$\overline{\gamma}_A$	Microrotation parameter
ε_0	Permittivity at vacuum
λ_0	Wavelength
μ_{0h}	Fluid viscosity
ν_s	Kinematic viscosity
ρ_s	Fluid density
ρ_n	Nanoparticle density
$(\rho c)_s$	Heat capacity of the fluid
$(\rho c)_n$	Heat capacity of nanoparticle
σ_s	Electrical conductivity
σ_0	Stefan Boltzmann coefficient
ω	Angle of tapering
$\underline{\tau}^h$	Cauchy stress tensor
F	Dimensionless nanoparticle phenomena
f	Nanoparticle phenomena
f_0	Nanoparticle at the left wall
f_1	Nanoparticle at the right wall
ξ	The second invariant strain tensor
$\psi(r,z)$	Stream function

Data availability

The datasets generated and/or analyzed during the current study are not publicly available due [All the required data are only with the corresponding author] but are available from the corresponding author on reasonable request.

References

[1] A. C. Eringen, Journal of Mathematical Mechanics, 16 (1966), 1-18.
[2] A. A. Dar, Peristaltic motion of micropolar fluid with slip velocity in A tapered asymmetric channel in presence of inclined

magnetic field and thermal radiation, *Sohag Journal of Mathematics*, **8** (1) (2021), 9-22.

[3] N. T. M. Eldabe, G. M. Moatimid, M. A. A. Mohamed and Y. M. Mohamed, A couple stress of peristaltic motion of Sutterby micropolar nanofluid inside a symmetric channel with a strong magnetic field and Hall currents effect, *Archive of Applied Mechanics*, **91** (2021), 3987 – 4010.

[4] D. Tripathi, J. Prakash, M. G. Reddy and J. C. Misra, Numerical simulation of double diffusive convection and electroosmosis during peristaltic transport of a micropolar nanofluid on an asymmetric microchannel, *Journal of Thermal Analysis and Calorimetry,* **143** (2021), 2499–2514.

[5] N. T. M. Eldabe and M.Y. Abou-zeid, Magnetohydrodynamic peristaltic flow with heat and mass transfer of micropolar biviscosity fluid through a porous medium between two co-axial tubes, *Arabian Journal for Science and Engineering*, **39** (2014), 5045–5062.

[6] J. C. Misra, S. Chandra, G. C. Shit and P. K. Kundu, Electroosmotic oscillatory flow of micropolar fluid in microchannels: application to dynamics of blood flow in microfluidic devices*, Applied Mathematics and Mechanics: - English Edition*, **35** (6) (2014), 749–766.

[7] Kh. S. Mekheimer and M. A. El Kot, The micropolar fluid model for blood flow through a tapered artery with a stenosis, *Acta Mechanica Sinica*, **24** (2008), 637–644.

[8] J. B. Fourier Theorie analytique, De La Chaleur: Paris, (1822).

[9] C. Cattaneo, Sulla conduzione del calore. Atti. Semin. Mat. Fis. Univ. *Modena Reggio Emilia*, **3** (1948), 89-101.

[10] C. L. Christov, On frame indifferent formulation of the Maxwell – Cattaneo model of finite – speed heat conduction, *Mechanics Research Communications*, **36** (2009), 481-486.

[11] N. T. M. Eldabe, M. Y. Abou-zeid, M. E. Oauf, D. R. Mostapha and Y. M. **Mohamed** Cattaneo – Christov heat and mass fluxes effect on MHD peristaltic transport of Bingham Al_2O_3 nanofluid through a non – Darcy porous medium, *International Journal of Applied Electromagnetics and Mechanics*, **68** (1) (2022), 59-84.

[12] A. Tanveer, S. Hina, T. Hayat and B. Ahmad, Effects of the Cattaneo–Christov heat flux model on peristalsis, *Engineering Applications of Computational Fluid Mechanics* **10** (1) (2016), 373–383.

[13] O. U. Mehmood, A. A. Qureshi, H. Yasmin and S. Uddin, Thermo-mechanical analysis of non-Newtonian peristaltic mechanism: modified heat flux model, *Physica A*, (2019), 1-21, doi: https://doi.org/10.1016/j.physa.2019.124014 .

[14] Z. W. Tong, S. U. Khan, H. Vaidya, R. Rajashekhar, T. Ch. Sun, M. I. Khan, K. V. Prasad, R. Chinram and A. A. Aly, Nonlinear thermal radiation and activation energy significances in slip flow of bioconvection of Oldroyd-B nanofluid with Cattaneo- Christov theories, *Case Studies in Thermal Engineering* **26** (2021), 1-12.

[15] M. A. Ahmad, L. B. McCash, Z. Shah and R. Nawaz, Cattaneo-Christov heat flux model for second grade nanofluid flow with Hall effect through entropy generation over stretchable rotating disk, *Coatings*, **10** (2020), 1-23.

[16] I. Ahmad, S. Aziz, S. U. Khan, and N. Ali, Periodically moving surface in an Oldroyd-B fluid with variable thermal conductivity and Cattaneo-Christov heat flux features, *Heat Transfer*, (2019), 1-21, doi: 10.1002/htj.21772.

[17] U. Nazir, M. Sohail, Al. H. Hussam, M. M. Selim, Ph. Thounthong and Ch. Park, Inclusion of hybrid nanoparticles in hyperbolic tangent material to explore thermal transportation via finite element approach engaging Cattaneo-Christov heat flux, *PLOS ONE*, (2021), 1-19, doi: https://doi.org/10.1371/journal.pone.0256302.

[18] N. T. M. Eldabe, G. M. Moatimid, M. A. A. Mohamed and Y. M. Mohamed, Effects of Hall currents with heat and mass transfer on the peristaltic transport of a Casson fluid through a porous medium in a vertical circular cylinder, *Thermal Science,* **24** (2B) (2020), 1067-1081.

[19] S. Das, B. N. Barman and R. N. Jana, Hall and ion-slip currents' role in transportation dynamics of ionic Casson hybrid nano-liquid in a microchannel via electroosmosis and peristalsis, *Korea-Australia Rheology Journal*, **33** (4) (2021), 367-391.

[20] P. Li, A. A. Abbasi, E. R. El-Zahar, W. Farooq, Z. Hussain, S. U. Khan, M. I. Khan, Sh. Farooq, M. Y. Malik, F. Wang., Hall effects and viscous dissipation applications in peristaltic transport of Jeffrey nanofluid

due to wave frame, *Colloid and Interface Science Communications,* **47** (2022), 1-13.

[21] Abou-zeid, M. Y. Magnetohydrodynamic boundary layer heat transfer to a stretching sheet including viscous dissipation and internal heat generation in a porous medium. J. porous Media. **14**, 1007-1018 (2011).

[22] M. Takashima and A. K. Ghosh, Electrohydrodynamic instability of viscoelastic liquid layer. *Journal of Physical Society of Japan*, **47** (1979), 1717-1722.

[23] El-Dabe, N.T., Abou-Zeid, M.Y. & Ahmed, O.S. Motion of a thin film of a fourth-grade nanofluid with heat transfer down a vertical cylinder: Homotopy perturbation method application. J. Adv. Res. Fluid Mech. Therm. Sci. 66, 101-113 (2020).

[24] Abouzeid, M.Y. Chemical reaction and non-Darcian effects on MHD generalized Newtonian nanofluid motion. Egy. J. Chem. 65, 647-655 (2022).

[25] M. M. Bhatti, A. Zeeshan, R. Ellahi, O. A. Bég and A. Kadir, Effects of coagulation on the two-phase peristaltic pumping of magnetized Prandtl biofluid through an Endoscopic annular geometry containing a porous medium, *Chinese Journal of Physics,* (2019) , 1-34, *doi:* https://doi.org/10.1016/j.cjph.2019.02.004.

[26] J. U. Abubakar and A. D. Adeoye, Effects of radiative heat and magnetic field on blood flow in an inclined tapered stenosed porous artery, *Journal of Taibah University for Science,* **14** (1) (2019), 77–86.

[27] N. T. Eldabe and D. R. Mostapha, MHD peristaltic flow of a Walter's-B fluid with mild stenosis through a porous medium in endoscope, *Journal of Porous Media,* **22** (9) (2019), 1109-1130.

[28] S. R. Shah and R. Kumar, Mathematical modeling of blood flow with the suspension of nanoparticles through a tapered artery with a blood clot, *Frontiers in Nanotechnology*, (2020), 1-5, doi: 10.3389/fnano.2020.596475.

[29] N. T. Eldabe and D. R. Mostapha, Hall current effects on electro-magneto-dynamic peristaltic flow of an Eyring–Powell fluid with mild stenosis through a uniform and non-uniform annulus, *Indian Journal of Physics,* (2021), 1-13, doi: https://doi.org/10.1007/s12648-021-02185-z.

[30] P. Devaki, B. Venkateswarlu, S. Srinivas and S. Sreenadh, MHD peristaltic flow of a nanofluid in a constricted artery for different shapes of nanosize particles, *Nonlinear Engineering*, **9** (2020), 51–59.

[31] M. Y. Abou-zeid, Effects of thermal - diffusion and viscous dissipation on peristaltic flow of micropolar non-Newtonian nanofluids: application of homotopy perturbation method, *Result in physics,* **6** (2016), 481-495.

[32] M. Y. Abou-zeid and M. A. A. Mohamed, Homotopy perturbation method for creeping flow of non-Newtonian Power-Law nanofluid in a nonuniform inclined channel with peristalsis, *Z. Naturforsch,* **72** ((10)a) (2017), 899–907.

[33] M. Y. Abou-zeid, Homotopy perturbation method to gliding motion of bacteria on a layer of power-law nanoslime with heat transfer, *Journal of Computational and Theoretical Nanoscience,* **12** (2015), 3605–3614.

[34] M. P. Mahesh and C. S. K. Raju, Convective conditions and dissipation on Tangent Hyperbolic fluid over a chemically heating exponentially porous sheet, *Nonlinear Engineering*; **8** (2019), 407–418.

[35] N. Verma and R. S. Parihar, Mathematical model of blood flow through a tapered artery with mild stenosis and hematocrit, *Journal of Modern Mathematical Statistics*, **4** (2010), 38-43.

[36] J. H. He, Homotopy perturbation technique, *Computer Methods in Applied Mechanics and Engineering,* **178** (1999), 257-262.

[37] N. T. Eldabe, M. Y. Abou-zeid, O. H. El-Kalaawy, S. M. Moawad and O.S Ahmed, Electromagnetic steady motion of Casson fluid with heat and mass transfer through porous medium past a shrinking surface, *Thermal Science,* **25** (1A) (2021), 257-265.

[38] M. El. Ouaf and M. Abou-zeid, Electromagnetic and non-Darcian effects on a micropolar non-Newtonian fluid boundary-layer flow with heat and mass transfer, *International Journal of Applied Electromagnetics and Mechanics,* **66** (2021), 693-703.

[39] N. T. M. Eldabe, M. Y. Abou-zeid, S. M. Elshabouri, T. N. Salama and A. M. Ismael, Ohmic and viscous dissipation effects on micropolar non-Newtonian nanofluid Al2O3 flow through a non-Darcy porous media, *International Journal of Applied Electromagnetics and Mechanics*, **68** (2022), 209-221.

[40] N. T. M. Eldabe, R. R. Rizkallah, M. Y. Abou-zeid and V. M. Ayad, Thermal diffusion and diffusion thermo effects of

Eyring- Powell nanofluid flow with gyrotactic microorganisms through the boundary layer, *Heat Transfer - Asian Research,* **49** (2020), 383 – 405.

[41] M. El. M. Ouaf and M. Y. Abou-zeid, Hall currents effect on squeezing flow of non-Newtonian nanofluid through a porous medium between two parallel plates, *Case Studies in Thermal Engineering,* **28** (2021), 101362.

[42] N. T. M. Eldabe, M. Y. Abou-zeid, M. A. A. Mohamed and M. M. Abd-Elmoneim, MHD peristaltic flow of non-Newtonian power-law nanofluid through a non-Darcy porous medium inside a non-uniform inclined channel, *Archive of Applied Mechanics,* **91** (2021), 1067–1077.

[43] M. Y. Abou-zeid, Implicit homotopy perturbation method for MHD non-Newtonian nanofluid flow with Cattaneo-Christov heat flux due to parallel rotating disks, *Journal of nanofluids,* **8** (8) (2019), 1648-1653.

[44] N. T. Eldabe, G. M. Moatimid, M. Y. Abouzeid, A. A. ElShekhipy and N. F. Abdallah, A semi analytical technique for MHD peristalsis of pseudoplastic nanofluid with temperature- dependent viscosity: Application in drug delivery system, *Heat Transfer-Asian Research,* **49** (2020), 424–440.

[45] N. T. M. Eldabe, G. M. Moatimid, M. Abou-zeid, A. A. Elshekhipy and N. F. Abdallah, Semi-analytical treatment of Hall current effect on peristaltic flow of Jeffery nanofluid, *International Journal of Applied Electromagnetics and Mechanics*, **7** (2021), 47-66.

[46] N. T. M. Eldabe, M. Y. Abou-zeid, A. Abosaliem, A. Alana, and N. Hegazy, Homotopy perturbation approach for Ohmic dissipation and mixed convection effects on non-Newtonian nanofluid flow between two co-axial tubes with peristalsis, *International Journal of Applied Electromagnetics and Mechanics*, **67** (2021), 153-163.

[47] N. T. Eldabe, M. Y. Abou-zeid, M. A. Mohamed and M. Maged, Peristaltic flow of Herschel Bulkley nanofluid through a non-Darcy porous medium with heat transfer under slip condition, *International Journal of Applied Electromagnetics and Mechanics*, **66** (2021), 649-668.

[48] N. T. M. Eldabe, G. M. Moatimid, M. Abou-zeid, A. A. Elshekhipy and N. F. Abdallah, Instantaneous thermal-diffusion and diffusion-thermo effects on Carreau nanofluid flow over a stretching porous sheet, *Journal of Advanced Research in Fluid Mechanics and Thermal Sciences,* **72** (2020) 142-157.

[49] N. T. Eldabe, A. A. Shaaban, M. Y. Abou-Zeid, H. A. Ali, Magnetohydrodynamic non-Newtonian nanofluid flow over a stretching sheet through a non-Darcy porous medium with radiation and chemical reaction, *Journal of Computational and Theoretical Nanoscience*, **12** (2015), 5363-5371.

[50] M. A. Mohamed and M.Y. Abou-zeid, MHD peristaltic flow of micropolar Casson nanofluid through a porous medium between two co-axial tubes*, Journal of porous media,* **22** (2019), 1079–1093.

[51] N T. Eldabe and M. Y. Abou-Zeid, Radially varying magnetic field effect on peristaltic motion with heat and mass transfer of a non-Newtonian fluid between two co-axial tubes, *Thermal Science*, **22** (6A) (2018), 2449-2458.

[52] N. T. M. Eldabe, M. A. Hassan and M. Y. Abou-Zeid, Wall properties effect on the peristaltic motion of a coupled stress fluid with heat and mass transfer through a porous medium, *Journal of Engineering Mechanics*, **142** (2016), (04015102-1) – (04015102-9).

[53] M.Y. Abou-zeid, Homotopy perturbation method for couple stresses effect on MHD peristaltic flow of a non-Newtonian nanofluid, *Microsystem Technologies*, **24** (2018), 4839–4846.

[54] N. T. M. Eldabe, R. R. Rizkallah, M. Y. Abou-zeid and V. M. Ayad, Effect of induced magnetic field on non-Newtonian nanofluid Al_2O_3 motion through boundary-layer with gyrotactic microorganisms, *Thermal Science*, **26** (2022), 411 – 422.

[55] N. T. M. Eldabe, M. Y. Abou-zeid, A. Abosaliem, A. Alana and N. Hegazy, Thermal diffusion and diffusion thermo effects on magnetohydrodynamics transport of non-Newtonian nanofluid through a porous Media between two wavy co-zxial tubes, *IEEE Transactions on Plasma Science*, **50** (2021), 1282-1290.

[56] N. T. Eldabe, S. Elshabouri, H. Elarabawy, M. Y. Abouzeid and A. J. Abuiyada, Wall properties and Joule heating effects on MHD peristaltic transport of Bingham non-Newtonian nanofluid, *International Journal of Applied Electromagnetics and Mechanics*, **69** (2022), 87 – 106.

[57] N.T. Eldabe, M.Y. Abou-zeid and H. A. Shawky, MHD peristaltic transport of Bingham blood fluid with heat and mass transfer through a non-uniform channel, J. Adv. Res. Fluid Mech. *Thermal Science*, **77** (2021), 145–159.

[58] A. Ismael, N. Eldabe, M. Abouzeid and S. Elshabouri, Activation energy and chemical reaction effects on MHD Bingham nanofluid flow through a non-Darcy porous media, *Egyptian Journal of Chemistry*, **65** (2022), 715 – 722.

[59] M. Ibrahim, N. Abdallah and M. Abouzeid, Activation energy and chemical reaction effects on MHD Bingham nanofluid flow through a non-Darcy porous media, Egyptian Journal of Chemistrey, **66**, 137 – 144 (2023).

[60] Ismael, A.M., Eldabe, N.T.M., Abouzeid, M.Y., & Elshabouri, S.M. Thermal micropolar couple stresses effects on peristaltic flow of biviscosity nanofluid through a porous medium. Scientific Reports **12**, 16180 (2022).

[61] Abouzeid, M.Y., & Ibrahim, M. G. Influence of variable velocity slip condition and activation energy on MHD peristaltic flow of Prandtl nanofluid through a non-uniform channel. Scientific Reports 12, 18747 (2022).

[62] Mansour, H. M. & Abouzeid, M. Y. Heat and mass transfer effect on non-Newtonian fluid flow in a non-uniform vertical tube with peristalsis. J. Adv. Res. Fluid Mech. Therm. Sci., 61, 44-64 (2019).

[63] Eldabe, N. T., Abouzeid, M. Y. Mohamed, M. A. A., Abd-Elmoneim, M. M. Peristaltic mixed convection slip flow of a Bingham nanofluid through a non-darcy porous medium in an inclined non-uniform duct with viscous dissipation and radiation. J. of Appl. Nonlinear Dyn. 12, 231-243 (2023).

[64] Abou-zeid, M. Y. Homotopy perturbation method to MHD non-Newtonian nanofluid flow through a porous medium in eccentric annuli with peristalsis Therm. Sci. 21, 2069 - 2080 (2015).

[65] Abuiyada, A. Eldabe, N. T., Abouzeid, M. Y. Elshabouri, S. Influence of Both Ohmic Dissipation and Activation Energy on Peristaltic Transport of Jeffery Nanofluid through a Porous Media, CFD Letters 15, Issue 6 (2023) 65-85.

[66] Eldabe, N.T., Abou-Zeid, M.Y. The wall properties effect on peristaltic transport of micropolar non-newtonian fluid with heat and mass transfer, Mathematical Problems in Engineering, 808062 (2010).

[67] Shaaban, A.A., Abou-Zeid, M.Y. Effects of heat and mass transfer on MHD peristaltic flow of a non-newtonian fluid through a porous medium between two coaxial cylinders, Mathematical Problems in Engineering, 819683 (2013).